Genetic characterisation of the *Theileria annulata* cytochrome b locus and its impact on buparvaquone resistance in ruminants

Qasim Ali[1], Osama Zahid[2], Moez Mhadhbi[5], Ben Jones[3], Mohamed Aziz Darghouth[5], George Raynes[2], Kiran Afshan[4], Richard Birtles[6], Neil D. Sargison[2], Martha Betson[3], Umer Chaudhry[3]*

1. Faculty of Veterinary and Animal Sciences, University of Agriculture, Dera Ghazi Khan, Pakistan.
2. Royal (Dick) School of Veterinary Studies, University of Edinburgh, UK
3. School of Veterinary Medicine, University of Surrey, UK
4. Department of Zoology, Faculty of Biological Sciences, Quaid-i-Azam University, Islamabad, Pakistan.
5. Laboratoire de Parasitologie, École Nationale de Médecine Vétérinaire, Université de la Manouba, Sidi Thabet, Tunisia.
6. School of Science, Engineering and Environment, University of Salford, UK

*Corresponding author:

Umer Chaudhry
Email: u.chaudhry@surrey.ac.uk, Tel: 00447490028661
School of Veterinary Medicine, University of Surrey, UK, GU2 7AL

Abstract

Control of tropical theileriosis depends on the use of a single drug, buparvaquone, the efficacy of which is compromised by the emergence of resistance. The present study was undertaken to improve understanding of the role of mutations conferring buparvaquone resistance in *Theileria annulata*, and the effects of selection pressures on their emergence and spread. First, we investigated genetic characteristics of the cytochrome b locus associated with buparvaquone resistance in 10 susceptible and 7 resistant *T. annulata* isolates. The 129G (GGC) mutation was found in the Q_{01} binding pocket and 253S (TCT) and 262S (TCA) mutations were identified within the Q_{02} binding pocket. Next, we examined field isolates and identified cytochrome b mutations 129G (GGC), 253S (TCT) and 262S (TCA) in 21/75 buffalo-derived and 19/119 cattle-derived *T. annulata* isolates, providing evidence of positive selection pressure. Both hard and soft selective sweeps were identified, with striking differences between isolates. For example, 19 buffalo-derived and 7 cattle-derived isolates contained 129G (GGC) and 253S (TCT) resistance haplotypes at a high frequency, implying the emergence of resistance by a single mutation. Two buffalo-derived and 11 cattle-derived isolates contained equally high frequencies of 129G (GGC), 253S (TCT), 129G (GGC)/253S (TCT) and 262S (TCA) resistance haplotypes, implying the emergence of resistance by pre-existing and or recurrent mutations. Phylogenetic analysis further revealed that 9 and 21 unique haplotypes in buffalo and cattle-derived isolates were present in a single lineage, suggesting a single origin. We propose that animal migration between farms is an important factor in the spread of buparvaquone resistance in endemic regions of Pakistan. The overall outcomes will be useful in understanding how drug resistance emerges and spreads, and this information will help design strategies to optimise the use and lifespan of the single most drug use to control tropical theileriosis.

Keywords: Buparvaquone, *Theilieria annulata*, resistance, soft selective sweep, hard selective sweep.

1. Introduction

Tropical theileriosis, caused by *Theileria annulata* and transmitted by *Hyalomma* ticks, is one of the most important livestock diseases in Asia and North Africa. The disease is highly pathogenic, infecting mononuclear cells of mammalian hosts (Nene et al., 2016). *T. annulata* has a major impact on food production in low- and middle-income countries throughout South Asia, the Middle East and North Africa, where efficient agriculture and livestock production is a priority under the UN Sustainable Development Goals. The disease causes severe economic losses due to high mortality and morbidity of livestock, having a significant impact on meat and milk production (Jabbar et al., 2015).

Hydroxynaphthoquinone drugs, including buparvaquone and atovaquone compounds, are widely used for the treatment of protozoan parasites of livestock and humans, respectively. These drugs bind to parasite cytochrome b, inhibiting mitochondrial respiration (Fry and Pudney, 1992; McHardy et al., 1983; McHardy and Morgan, 1985; McHardy et al., 1985). Different studies have shown associations between resistance to atovaquone in *Plasmodium* and *Toxoplasma* species and mutations in cytochrome b catalytic Q_{01} (codon 129-148), and oxidative Q_{02} (codon 244-266) binding pockets (Kessl et al., 2005; Kessl et al., 2006; Kessl et al., 2007; Korsinczky et al., 2000; Schwobel et al., 2003; Song et al., 2015; Srivastava et al., 1999). Atovaquone resistance-associated cytochrome b mutations at codon 268 have been reported in *Plasmodium falciparum* (David et al., 2003; Farnert et al., 2003; Fivelman et al., 2002; Musset et al., 2006; Schwartz et al., 2003); mutations at codon 133, 144 and 284 in *Plasmodium berghei* (Siregar et al., 2008; Syafruddin et al., 1999); and mutations at codon 129 and 254 in *Toxoplasma gondii* (McFadden et al., 2000).

The control of theileriosis heavily depends on the use of buparvaquone; it is the only effective commercially available drug for use in livestock. Clinical cases of buparvaquone resistance have been reported and represent a serious threat to efficient livestock production (Cui et al., 2015; Mhadhbi et al., 2010; Muraguri et al., 2006). Current understanding of the mechanism of buparvaquone resistance in *T. annulata* is limited, albeit links between mutations in cytochrome b and the resistance phenotype have been demonstrated (Mhadhbi et al., 2015). Moreover, a few studies have demonstrated buparvaquone resistance-associated mutations at codon 129, 253 and 262 in *T. annulata* isolates collected from Iran (Sharifiyazdi et al., 2012), Tunisia (Mhadhbi et al., 2015) and Sudan (Chatanga et al., 2019).

Selective sweep models could potentially explain how resistance mutations emerge in parasites; whereby the use of antiparasitic drugs provides positive selection pressure for adaptive mutations in the resistance candidate loci of the parasite (Chaudhry and Gilleard, 2015). A hard selective sweep is characterised by a single resistance haplotype rising from a recent mutation at a high frequency in each parasite isolate (Chaudhry et al., 2020; Chaudhry et al., 2015; Shaukat et al., 2019). A soft selective

sweep is characterised by the presence of multiple resistance haplotypes at a high frequency in each isolate, derived from either recurrent mutations appearing after the onset of selection, or pre-existing mutations before the onset of selection (Chaudhry et al., 2016a; Chaudhry et al., 2020; Shaukat et al., 2019). Understanding adaptive mutations in response to selection can help to determine their origin and spread (Chaudhry and Gilleard, 2015). For example, phylogenetic models might imply that new resistance mutations could arise from a single origin, become fixed by selection and then spread through parasites by migration. This scenario would likely be a consequence of the gene flow of drug resistance alleles through host movement. In contrast, resistance mutations could repeatedly arise from multiple origins, become fixed by selection and migrate between parasites as a result of host movement (Chaudhry et al., 2016a; Chaudhry et al., 2015; Shaukat et al., 2019; Shaukat et al., 2021).

High throughput deep amplicon sequencing using the Illumina Mi-Seq platform is an accurate and relatively low-cost method for the identification of amplicon sequence variants in parasites. The method has transformed the study of benzimidazole resistance in nematode parasites (Ali et al., 2019; Sargison et al., 2019), and pyrimethamine resistance in *Plasmodium* (Shaukat et al., 2019; Shaukat et al., 2021) and has the potential to open new areas of research to improve understanding of buparvaquone resistance in *Theileria*. The method can generate sequence reads up to 600 bp in length by targeting primer binding to conserved sites. Moreover, with the use of barcoded primers, up to 384 samples can be pooled and sequenced in a single Mi-Seq run.

The overall aim of the present study was to develop a genetic approach to improve understanding of the *T. annulata* cytochrome b locus in buparvaquone resistance. This allowed the analysis of alleles conferring resistance and susceptibility to investigate different models of emergence and the spread of associated mutations. The specific objectives were: (i) To characterise single nucleotide polymorphism (SNPs) in the cytochrome b locus and their genetic role in buparvaquone resistance in *T. annulata*. (ii) To investigate the consequences of selection pressure on the emergence and spread of *T. annulata* cytochrome b resistance-conferring mutations in the field isolates. Overall, the results will lead to an increased understanding of buparvaquone resistance in an important tropical livestock pathogen, with the potential to inform enhanced animal health, improved global food security, and poverty alleviation through reduced production losses.

2 Materials and methods

2.1. Buparvaquone susceptible and resistant T. annulata isolates

Four infected cell lines (TA-ank, TA-but, TA-has, TA-mor) had been produced by the infection of blood mononuclear cells with laboratory-maintained stocks of *T. annulata* held in the Roslin Institute of the University of Edinburgh, originally isolated in Turkey, India, Tunisia, and Morocco (Katzer et al., 1994). The stock was selected to represent buparvaquone susceptible isolates. Genomic DNA of

was prepared using 1,000 µl Direct PCR lysis reagent (Viagen), 50 µl proteinase K solution (Qiagen), and 50 µl 1M dithiothreitol (DTT). To extract the gDNA, 50 µl of each isolate was transferred into a fresh tube and centrifuged for 5 minutes, before removing the supernatant and mixing with 25 µl lysis buffer (Viagen), Proteinase K (New England BioLabs) and dithiothreitol (DTT).

Six known buparvaquone susceptible isolates (674, Battan C, Battan P4, Chargui P5, Jed4, Jed4 P10) were selected from different endemic regions in the north-east of Tunisia. Battan C, Battan P4, Jed4 P10 and Jed4 isolates were chosen based on previous studies confirming the susceptibility of these stocks to buparvaquone (Darghouth et al., 1996). The Chergui P5 and 674 isolates were chosen from the animals cured after the first injection of buparvaquone. Seven known buparvaquone resistant isolates (ST2/13, ST2/19, 739, 881III, 5911, 8307, BC2T) were selected from different endemic regions in the north-east of Tunisia. Two buparvaquone resistant isolates (ST2/13, ST2/19) were taken from the previous study by Mhadhbi *et al* (2015). Resistant stocks ST2/13 and ST2/19 were isolated from a clinical case of treatment failure against tropical theileriosis using buparvaquone. The samples were collected at different times after treatment as follows: isolate ST2/13 was taken 24 hours after the first treatment and the ST2/19 isolate was taken 48 hours after the third treatment (Mhadhbi et al., 2015). Five stocks (739, 881III, 5911, 8307, BC2T) were initially isolated at various times points from tropical theileriosis clinical cases of treatment failure based on the absence of clinical improvement despite the early initiation of treatment with the conventional dose of buparvaquone, and the persistence of a high parasitaemia after at least three doses of buparvaquone. All isolates were collected by lymph node punctures or from whole blood and cultured in a complete RPMI 1640 medium. They had been used at the low passage to avoid *in-vitro* pressure selection (Mhadhbi et al., 2015). Genomic DNA was extracted using a Promega Wizard DNA Purification kit (Madison, WI, USA) according to the manufacturer's instructions.

2.2. Theileria annulata field isolates

Field isolates were taken from suspected piroplasm infected cattle and buffalo presented at veterinary clinics across the endemic regions of Pakistan between 2020 and 2021. Moreover, piroplasm-negative cattle blood samples were provided by Dr Tim Connelly, Roslin Institute, University of Edinburgh. The samples were collected by para-veterinary staff under the supervision of local veterinarians following consent from the animal owners. The study was approved by the Institutional Review Board of the Quaid-i-Azam University Islamabad Pakistan (No. #BEC-FBS-QAU2017). Peripheral blood smears were prepared and stained with 4% Giemsa and examined microscopically to detect piroplasms. Genomic DNA was isolated from positive samples by lysis with GS buffer containing proteinase K as described in the TIANamp Blood DNA Kit (TIANGEN Biotech Co. Ltd, Beijing) and stored at -20°C. 'Haemoprotobiome' high-throughput sequencing was performed

on piroplasm-positive blood samples to confirm the presence of *T. annulata* as previously described (Chaudhry et al., 2019). Briefly, 194-piroplasm positive field samples [buffalo (n=75), cattle (n=119)] were examined to identify the species of *T. annulata* involved in the infections.

2.3. PCR amplification, Illumina Mi-Seq run and bioinformatics data handling of cytochrome b locus

A 516 bp fragment of the cytochrome b locus of *T. annulata* laboratory and field isolates was amplified. The primer sets, adapter/barcoded PCR amplification conditions and magnetic bead purification were previously described by Chaudhry et al. (2021) (Supplementary Table S1 and S2). Ten µl of each barcoded bead purified PCR product were combined to make a pooled library which was subject to agarose gel electrophoresis. Cytochrome b products were excised and purified from the gel using a commercial kit (QIAquick Gel Extraction Kit, Qiagen, Germany), followed by purification of eluted DNA using AMPure XP Magnetic Beads (1X) (Beckman Coulter, Inc.). Purified products were then combined into a single purified DNA pool library. The library was quantified with qPCR library quantification kit (KAPA Biosystems, USA) and then run on an Illumina MiSeq Sequencer using a 600-cycle pair-end reagent kit (MiSeq Reagent Kits v2, MS-103-2003) at a concentration of 15nM with the addition of 15% Phix Control v3 (Illumina, FC-11-2003) described by Chaudhry et al. (2021).

The Illumina Mi-Seq post-run processing uses the barcoded indices to separate all sequences by sample and generate FASTQ files. The FASTQ files of the buparvaquone susceptible and resistant *T. annulata* isolates and *T. annulata* field isolates have been made freely available through the Mendeley database (doi: 10.17632/n6xpdcntvf.1). These files were analysed using Mothur v1.39.5 software (Kozich et al., 2013; Schloss et al., 2009) with modifications in the standard operating procedures of Illumina Mi-Seq in the Command Prompt pipeline described by Chaudhry et al. (2021).

2.4. Allele frequency of buparvaquone resistance-associated SNPs in the cytochrome b locus

The calculation of the relative allele frequencies of *T. annulata* cytochrome b resistance-associated mutations identified in the buparvaquone susceptible and resistant isolates and field isolates was performed by dividing the number of sequence reads of each isolate by the total number of reads (R Core Team, 2013; package ggplot2).

2.5. Genetic models of buparvaquone resistance-associated SNPs in the cytochrome b locus

The sequence reads of the *T. annulata* cytochrome b locus from each isolate were imported into the FaBox 1.5 tool (birc.au.dk) to collapse the sequences that showed 100% base pair similarity after corrections into a single haplotype (freely available through the Mendeley database doi: 10.17632/n6xpdcntvf.1). The haplotypes of cytochrome b were then aligned using the MUSCLE

alignment tool in Geneious v10.2.5 software (Biomatters Ltd, New Zealand) for the analysis of the emergence of buparvaquone resistance-associated mutations in the cytochrome b locus. The haplotypes of the *T. annulata* cytochrome b locus were selected for neutrality analysis. Tests for selective neutrality were analysed to determine whether the observed frequency distribution of sequence polymorphism in *T. annulata* cytochrome b locus departed from neutral expectations using the DnaSP 5.10 software package (Librado and Rozas, 2009). The neutrality tests included Tajima's D (Tajima, 1989) and Fay & Wu's H (Fay and Wu, 2000) methods.

A split tree of cytochrome b haplotypes was created in the SplitTrees4 software (bio-soft.net) using the neighbour-joining method and the JukesCantor model of substitution. The appropriate model of nucleotide substitutions for neighbour-joining analysis was selected by using the jModeltest 12.2.0 program (Posada, 2008). The network tree of *T. annulata* cytochrome b haplotypes was produced based on the neighbour-joining algorithm built on a sparse network and the epsilon parameter is set to zero default in Network 4.6.1 software (Fluxus Technology Ltd.). All unnecessary median vectors and links were removed with the star contractions. The number of mutations separating adjacent sequence nodes was indicated along connecting branches and the length of the lines connecting the haplotypes is proportional to the number of nucleotide changes.

3. Results

3.1. Buparvaquone resistance-associated SNPs in susceptible and resistant T. annulata isolates

A 516 bp region of the cytochrome b locus corresponding to the buparvaquone binding pockets [(Q_{01} (codon 129-148) and Q_{02} (codon 244-266)] of the susceptible and resistant *T. annulata* isolates was selected for deep amplicon sequencing. The sequences of 10 susceptible and 7 resistant isolates were compared. Eleven point mutations in the *T. annulata* cytochrome b locus were found at codons A133V (GCT/GTT), V135F (GTC/TTC), I136L (ATA/CTA), G138V (GGT/GTT), L139F (TTG/TTT), L140F (TTG/TTT), K141N (AAA/AAC), F143L (GGA/GTA), G144V (GGA/GTA) and T146A (ACT/GCT), within the cytochrome b Q_{01} binding pocket. These SNPs were present at similar frequencies across the buparvaquone susceptible and resistant *T. annulata* isolates (Table 1). One point mutation was found in the Q_{01} binding pocket at codon 129G (GGC) in resistant isolates compared to S129 (AGC) in susceptible isolates (Table 1). Similarly, two-point mutations were found within the Q_{02} binding pocket at codons 253S (TCT) and 262S (TCA) in resistant isolates compared to P253 (CCT) and L262 (TTA) in susceptible isolates (Table 1). Overall, the results provide a comprehensive analysis of cytochrome b mutations potentially involved in the development of buparvaquone resistance and the first genetic link between mutations and drug resistance in *T. annulata*.

3.2. Buparvaquone resistance-associated SNPs in buffalo- and cattle-derived T. annulata field isolates and their impact on positive selection pressure

A 516 bp fragment of the *T. annulata* cytochrome b locus was amplified from 75 buffalo-derived and 119 cattle-derived isolates across the endemic regions of Pakistan (Supplementary Table S3). The relative allele frequencies of three mutations S129G (AGC/GGC), P253S (CCT/TCT) and L262S (TTA/TCA) correspond to the buparvaquone binding pockets were determined. Buparvaquone resistance-associated mutations 129G (GGC), 253S (TCT) and 129G (GGC)/253S (TCT) were present in 21/75 buffalo-derived *T. annulata* (Fig. 1, Table 2). The 129G (GGC) mutation was present at frequencies of 4.3-100%. The 253S (TCT) mutation was present at frequencies of 19.2-27.3%. Conversely, 129G (GGC)/253S (TCT) double mutations were detected at frequencies of 1.3-4.3%. 262S (TCA) was not detected in any buffalo-derived *T. annulata* isolates (Fig. 1, Table 2). In contrast, buparvaquone resistance-associated mutations 129G (GGC), 253S (TCT) and 262S (TCA) were present in 19/119 cattle-derived *T. annulata* isolates (Fig. 1, Table 2). The 129G (GGC) mutation was present at frequencies of 1.4-100%. 253S (TCT) mutation was present at frequencies between 3.9-43%. 262S (TCA) mutation was detected at frequencies of 2.6-13.7%. 129G (GGC)/253S (TCT) was not detected in any cattle-derived *T. annulata* (Fig. 1, Table 2). Overall, the results indicated the positive selection pressure on the cytochrome b locus of 21 buffalo-derived and 19 cattle-derived *T. annulata* isolates.

3.3. Nature of selective sweeps associated with the emergence of cytochrome b resistance-associated SNPs in Buffalo- and cattle-derived T. annulata field isolates

The analysis of 21 buffalo-derived *T. annulata* revealed that 18 isolates contained the 129G (GGC) resistance haplotype and one isolate (CY110-B) contained the 253S (TCT) resistance haplotype at a high frequency of 100% (Fig. 2A, Table 3), providing evidence of hard selective sweep patterns. In contrast, the CY321-B isolate contained resistance haplotypes of 129G (GGC) at a frequency of 24.5%, 253S (TCT) at a frequency of 59.9% and 129G (GGC)/253S (TCT) at a frequency of 13.8% (Fig. 2A, Table 3). The CY322-B isolate contained resistance haplotypes of 129G (GGC) at a frequency of 14.4%, 253S (TCT) at a frequency of 79.3% and 129G (GGC)/253S (TCT) at a frequency of 4.6% (Fig. 2A, Table 3). These two isolates had equally high frequencies of cytochrome b resistance-conferring haplotypes demonstrating evidence of soft selective sweep patterns. Neutrality analysis further revealed a significant departure of neutrality in those 2 isolates providing evidence of a signature of selection at the *T. annulata* cytochrome b locus (Table 3).

The analysis of 19 cattle-derived *T. annulata* isolates revealed that 6 (CY212-C, 252-C, 258-C, 6-C, 43-C, 136-C) contained 129G (GGC) resistance haplotypes and one isolate (CY26-C) contained 253S

(TCT) resistance haplotype at a high-frequency of 100% (Fig. 2B, Table 3), demonstrating evidence of hard selective sweep patterns. In contrast, 9 isolates (CY268-C, 270-C, 272-C, 277-C, 38-C, 39-C, 40-C, 41-C, 42-C) contained 129G (GGC) resistance haplotypes and one isolate (CY150-C) contained 253S (TCT) resistance haplotypes at frequencies ranging between 16 to 84% (Fig. 2B, Table 3). The CY235-C isolate contained resistance haplotypes of 129G (GGC) at a frequency of 34.2% and 262S (TCA) at a frequency of 60.6%. The CY90-C isolate contained resistance haplotypes of 129G (GGC) at a frequency of 69.8%, 253S (TCT) at a frequency of 22.6% and 262S (TCA) at a frequency of 0.07% (Fig. 2B, Table 3). These 12 isolates had equally high frequencies of cytochrome b resistance-conferring haplotypes demonstrating evidence of soft selective sweep patterns. Neutrality analysis further revealed a significant departure of neutrality in 9 out of 12 isolates providing evidence of a signature of selection at the *T. annulata* cytochrome b locus (Table 3).

3.4. Phylogeny of cytochrome b resistance-associated SNPs in buffalo- and cattle-derived T. annulata field isolates and their impact on the origin and spread of buparvaquone resistance

The analysis of 21 buffalo-derived *T. annulata* revealed 22 unique cytochrome b haplotypes. Six haplotypes encoded 129G (GGC) resistance mutations, 2 haplotypes encoded 253S (TCT) resistance mutations, one haplotype encoded 129G (GGC)/253S (TCT) double resistance mutations and 13 haplotypes encoded S129 (AGC), P253 (CCT) and L262 (TTA) susceptible mutations (Fig. 3A, Fig. 4A, Table 3). A split tree analysis showed that 129G (GGC) resistance mutants and 129G (GGC)/253S (TCT) resistance mutants carried 7 haplotypes and 253S (TCT) resistance mutant carried 2 haplotypes were located in a single lineage demonstrating evidence of a single origin. (Fig. 3A). The network analysis showed that the BHA5-129G haplotype was present at a high frequency in eight different isolates collected from the livestock farms in the Okara and Gujranwala regions. The BHA7-129G haplotype was present in ten different isolates collected from the livestock farms in the Okara, Gujranwala, Vehari and Bahawalpur regions. BHA9-129G and BHA13-129G/253S haplotypes were present in two isolates collected from the livestock farms in the Gujranwala region. BHA2-253S haplotype was present in three isolates and BHA11-253S haplotype was present in two isolates collected from the livestock farms in the Gujranwala region (Fig 4A). The data provide evidence of a high level of gene flow, predicted to occur due to the unregulated animal movement. However, three haplotypes (BHA14-129G, BHA16-129G and BHA21-129G) were present at a frequency of 100% in a single isolate collected from the livestock farms in the Gujranwala region (Fig 4A), indicating that the resistance of those haplotypes had not yet spread.

The analysis of 19 cattle-derived *T. annulata* revealed 61 unique cytochrome b haplotypes. 12 haplotypes encoded 129G (GGC) resistance mutations, 6 haplotypes encoded 253S (TCT) resistance mutations, 3 haplotypes encoded 262S (TCA) resistance mutations and 40 haplotypes encoded S129

(AGC), P253 (CCT) and L262 (TTA) susceptible mutations (Fig. 3B, Fig. 4B, Table 3). A split tree analysis showed that 129G (GGC), 253S (TCT) and 262S (TCA) resistance mutants carried 10, 5 and 2 haplotypes were located in a single lineage (Fig. 3B) demonstrating evidence of a single origin (Fig. 3B). The network tree analysis showed that CHA4-129G haplotype was present at a high frequency in 7 different isolates collected from the livestock farms in the Gujranwala and Qadirabad regions. The CHA9-129G haplotype was present in 9 different isolates collected from the livestock farms in the Bahawalpur, Qadirabad, Vehari and Lodhran regions. CHA10-129G haplotype was present in 3 isolates, CHA12-129G in 2 isolates, CHA22-129G in 5 isolates at high frequency collected from the livestock farms in the Gujranwala, Qadirabad, Vehari and Okara regions. The analysis further revealed that CHA28-253S haplotype was present in two different isolates collected from the livestock farms in the Gujranwala and Vehari regions. CHA39-253S haplotype was present in three different isolates collected from the livestock farms in the Vehari and Okara regions (Fig 4B). The data of those 7 haplotypes demonstrate the evidence of a high level of gene flow, predicted to occur due to unregulated animal movement. Seven haplotypes (CHA15-129G, CHA16-129G, CHA18-129G, CHA37-129G, CHA41-129G, CHA44-129G, CHA45-129G) were present at a frequency of 100% in five isolates collected from the livestock farms in the Gujranwala, Qadirabad, Vehari and Okara regions (Fig 4B). Four haplotypes (CHA5-253S, CHA24-253S, CHA27-253S, CHA39-253S) were present at a frequency of 100% in single isolates collected from the livestock farms in the Gujranwala and Okara regions (Fig 4B). CHA38-262S, CHA52-262G, CHA58-262S haplotypes were present at a frequency of 100% in single isolates collected from the livestock farms in the Okara and Lodhran regions (Fig 4B). These data demonstrate that the resistance of these haplotypes was not spread yet.

4. Discussion

Buparvaquone has been widely used for the therapy of tropical theileriosis for nearly 30 years. The drug was introduced in the early 1990s and exerts its antiprotozoal actions against *T. annulata*. Buparvaquone resistance in *T. annulata* emerged in 2010 (Mhadhbi et al., 2010). The determinants of resistance to buparavaquone are probably complex in *T. annulata*, evidence suggest that mitochondrial and non-mitochondrial pathways contribute in *T. annulata* resistance to buparvaquone. Indeed, Marsolier et al. 2015 demonstrated that buparvaquone is targeting *Theileria* peptidyl prolyl isomerase to block the signalling pathways leading to the cells proliferations. Interestingly, this enzyme is mutated in a drug resistant isolates (Marsolier et al., 2015). In contrast, the present study is focusing on the mitochondrial pathway for buparvaquone resistance in *T. annulata*. The drug target the cytochrome bc_1 complex, inhibiting mitochondrial respiration (Fry and Pudney, 1992). The current understanding of the mechanism of resistance is limited, few studies have demonstrated buparvaquone resistance-associated mutations In *T. annulata* isolates (Chatanga et al., 2019; Mhadhbi et al., 2015; Sharifiyazdi

et al., 2012). There is a clear need to understand how the resistance mutations against buparvaquone drugs emerge. The frequency with which buparvaquone resistance in *T. annulata* arises and the extent to which it spreads are important considerations for its prevention and control. Therefore, the present study investigates the genetic characteristics of the cytochrome b locus and their impact on the buparvaquone resistance in ruminants. The study further describes genetic models to understand the emergence and spread of buparvaquone resistance at the cytochrome b locus of *T. annulata*.

Deep amplicon sequencing identified fourteen mutations in the cytochrome b catalytic Q_{01} and oxidative Q_{02} binding pockets of *T. annulata* collected from clinical cases of treatment failure in the endemic region of Tunisia. Eleven mutations were present at similar frequencies across the buparvaquone susceptible and resistant *T. annulata* isolates. One mutation at codon 129G (GGC) in resistant isolates and S129 (AGC) in susceptible isolates was found in the Q_{01} binding pocket. Similarly, two mutations at codons 253S (TCT) and 262S (TCA) in resistant isolates and P253 (CCT) and L262 (TTA) in susceptible isolates were found within the Q_{02} binding pocket. Similar studies have been shown that the same mutations in the cytochrome b locus of *T. annulata* isolate collected from clinical cases of treatment failure in Iran (Sharifiyazdi et al., 2012) and Tunisia (Mhadhbi et al., 2015) and Sudan (Chatanga et al., 2019). Overall, the data provide a comprehensive high throughput sequencing analysis of cytochrome b loci involved in the development of buparvaquone resistance and the first genetic link between mutations and drug resistance in *T. annulata*.

Deep amplicon sequencing was then performed to analyse the cytochrome b locus of buffalo- and cattle-derived *T. annulata* field isolates collected from the endemic regions of Pakistan. Buparvaquone resistance-associated mutations 129G (GGC), 253S (TCT) and 129G (GGC)/253S (TCT) were identified in 21 buffalo-derived and 19 cattle-derived *T. annulata* isolates. Overall, buparvaquone resistance-associated SNPs were reported for the first time in buffalo- and cattle-derived *T. annulata* field isolates and their impact on positive selection pressure. Our results are consistent with the study of the pyrimethamine resistance mutations in the protozoan parasite *Plasmodium vivax* (Auliff et al., 2006; Brega et al., 2004; de Pecoulas et al., 1998; Hastings et al., 2005; Imwong et al., 2003; Kaur et al., 2006; Kuesap et al., 2011; Lu et al., 2012; Mint Lekweiry et al., 2012; Ranjitkar et al., 2011; Schunk et al., 2006; Shaukat et al., 2019) and diminazene resistance in the *Trypanosoma brucei* (Carter et al., 1999; Mäser et al., 1999; Matovu et al., 2001). A possible explanation for the differences in the frequency of buparvaquone-conferring mutations with positive selection pressure may be variable drug doses, for example, if the 262S (TCA), 253S (TCT) and 129G (GGC)/253S (TCT) resistance mutations may be selected at low doses of buparvaquone, while 129G (GGC) may occur at higher doses. Overall, the data provide novel information for screening field samples for the detection of buparvaquone resistance mutations for example, in multiple isolates across different geographical regions. The information will aid in understanding how resistance mutations differ between

geographical locations with implications for decision-making tools for farmers, farm advisers and veterinarians to design parasite control regimes for individual flocks.

Both hard and soft selective sweep patterns have been demonstrated in the buparvaquone resistance mutations in *T. annulata* in the present study. A single resistance haplotype at a high frequency was detected in the 19 buffalo-derived and 18 cattle-derived isolates. The selective sweeps on these individual isolates were effectively harder with no evidence of a genetic footprint of selection detected by significant departures from the neutrality test. In contrast, multiple resistance haplotypes were detected at high frequencies in the 2 buffalo-derived and 11 cattle-derived isolates. The selective sweep on these individual isolates was effectively softer and a genetic footprint of selection was also detected by significant departures from the neutrality test. The results are consistent with the hypothesis that single and multiple mutations in dhfr locus emerged in the human protozoan parasite *P. vivax* (Shaukat et al., 2019). Overall, the data provide novel information on single and or multiple emergences of resistance mutations in this group of parasites that may have implications for targeted selective treatment, or use of different drug combinations, including new drugs or the modification of current compounds in resistance mitigation strategies.

It will be challenging to determine the emergence of resistance mutations with multiple haplotypes, either due to pre-existing mutations before the onset of positive selection or recurrent mutations after the onset of positive selection (Chaudhry and Gilleard, 2015). If the pre-existing mutations were the only source for the emergence of resistance, similar haplotypes would be present in the isolates (Chaudhry et al., 2016b), for example in the present study, 2 buffalo-derived isolates (CY321-B and CY322-B) carried four similar resistance haplotypes (BHA2-253S, BHA9-129G, BHA11-253S, BHA13-129G/253S). This striking similarity between the isolates provides evidence for the emergence of resistance by pre-existing mutations. If the recurrent mutations were the only source for the emergence of resistance mutations, different haplotypes would be present in the isolates (Chaudhry et al., 2016b), for example in the present study, 11 cattle-derived isolates have dramatically carried different haplotypes. This striking difference between the isolates provides evidence for the emergence of resistance by recurrent mutations.

In the present study, buffalo-derived 9 unique haplotypes of the 129G (GGC), 253S (TCT) resistance mutant and 129G (GGC)/253S (TCT) double resistance mutant were present in a single lineage, suggesting that there is a single origin of this mutation in *T. annulata* isolates examined. Similarly, 21 unique cattle-derived haplotypes of the 129G (GGC), 253S (TCT) and 262S (TCA) resistance mutant demonstrated evidence of a single origin. These results contrast with those of a previous study of the evolutionary origin of human protozoan parasite *P.vivax* dhfr resistance-conferring mutations demonstrated evidence of a single origin of pyrimethamine resistance (Shaukat et al., 2021).

In the present study, 129G (GGC), 253S (TCT) and 129G (GGC)/253S (TCT) and 262S (TCA) mutations were present in buffalo- and cattle-derived *T. annulata* collected from different livestock farms in the endemic regions and their phylogenetic relationship suggests that there is a high level of gene flow, possibly occuring due to unregulated animal movement. Notably, the two resistance haplotypes of the 129G (GGC) mutation predominate in 8 and 10 buffalo-derived *T. annulata* isolates and the other four resistance haplotypes of 129G (GGC), 253S (TCT) and 129G (GGC)/253S (TCT) mutations were present in 2 and 3 buffalo-derived *T. annulata* isolates respectively. In cattle-derived *T. annulata*, six resistance haplotypes of the 129G (GGC) mutation predominate between 7 to 10 different isolates and the other two resistance haplotypes of 129G (GGC) and 253S (TCT) mutations were present in 2 and 3 different isolates respectively. Overall, the unregulated animal movement has likely contributed to the spread of buparvaquone resistance haplotypes in the endemic region of Pakistan. The spread of resistance mutations may require a degree of reproductive isolation of the hosts and parasites with resistant alleles.

5. Conclusion

There are limited studies which have undertaken a genetic characteristic to detect buparvaquone resistance mutations in *T. annulata* of ruminant livestock under natural field conditions. Therefore, the data obtained in the present study provide a comprehensive analysis of whether cytochrome b loci are involved in the development of buparvaquone resistance and the first link between genetic mutations and drug resistance in *T. annulata*. There has been no study investigating the emergence of buparvaquone resistance in *T. annulata* and it is still unclear how resistance mutations spread in parasite populations under natural field conditions. The data then obtained in the present study provide information on single and or multiple emergences of resistance mutations and their spread models could have implications for novel buparvaquone resistance mitigation strategies.

Acknowledgements

The study was financially supported by the Carnegie Trust Scotland and Biotechnology and Biological Sciences Research Council (BBSRC). Work at the Qaid-i-Azam University Pakistan and the University of Agriculture, Dera Ismail Khan Pakistan uses facilities funded by the Higher Education Commission of Pakistan.

References

Ali, Q., Rashid, I., Shabbir, M.Z., Aziz Ul, R., Shahzad, K., Ashraf, K., Sargison, N.D., Chaudhry, U., 2019. Emergence and the spread of the F200Y benzimidazole resistance mutation in Haemonchus contortus and Haemonchus placei from buffalo and cattle. Veterinary Parasitology 265, 48-54.

Auliff, A., Wilson, D.W., Russell, B., Gao, Q., Chen, N., Anh le, N., Maguire, J., Bell, D., O'Neil, M.T., Cheng, Q., 2006. Amino acid mutations in Plasmodium vivax DHFR and DHPS from several geographical regions and susceptibility to antifolate drugs. Am J Trop Med Hyg 75, 617-621.

Brega, S., de Monbrison, F., Severini, C., Udomsangpetch, R., Sutanto, I., Ruckert, P., Peyron, F., Picot, S., 2004. Real-time PCR for dihydrofolate reductase gene single-nucleotide polymorphisms in Plasmodium vivax isolates. Antimicrob Agents Chemother 48, 2581-2587.

Carter, N.S., Barrett, M.P., de Koning, H.P., 1999. A drug resistance determinant in Trypanosoma brucei. Trends in microbiology 7, 469-471.

Chatanga, E., Mosssad, E., Abdo Abubaker, H., Amin Alnour, S., Katakura, K., Nakao, R., Salim, B., 2019. Evidence of multiple point mutations in Theileria annulata cytochrome b gene incriminated in buparvaquone treatment failure. Acta Trop 191, 128-132.

Chaudhry, U., Ali, Q., Rashid, I., Shabbir, M.Z., Ijaz, M., Abbas, M., Evans, M., Ashraf, K., Morrison, I., Morrison, L., Sargison, N.D., 2019. Development of a deep amplicon sequencing method to determine the species composition of piroplasm haemoprotozoa. Ticks Tick Borne Dis 10, 101276.

Chaudhry, U., Ali, Q., Zheng, L., Rashid, I., Shabbir, M.Z., Numan, M., Ashraf, K., Evans, M., Rafiq, S., Oneeb, M., Morrison, L.J., Ivan Morrison, W., Sargison, N.D., 2021. Contrasting population genetics of co-endemic cattle- and buffalo- derived Theileria annulata. Ticks Tick Borne Dis 12, 101595.

Chaudhry, U., Gilleard, J., 2015. Molecular Analysis of Benzimidazole Resistance in Haemonchus contortus and Haemonchus placei. PhD Thesis

Chaudhry, U., Redman, E., Ashraf, K., Shabbir, M.Z., Rashid, M.I., Ashraf, S., Gilleard, J.S., 2016a. Microsatellite marker analysis of Haemonchus contortus populations from Pakistan suggests that frequent benzimidazole drug treatment does not result in a reduction of overall genetic diversity. Parasites & vectors 9, 349.

Chaudhry, U., Redman, E.M., Ashraf, K., Shabbir, M.Z., Rashid, M.I., Ashraf, S., Gilleard, J.S., 2016b. Microsatellite marker analysis of Haemonchus contortus populations from Pakistan suggests that frequent benzimidazole drug treatment does not result in a reduction of overall genetic diversity. Parasites & Vectors 9, 349.

Chaudhry, U., Redman, E.M., Kaplan, R., Yazwinski, T., Sargison, N., Gilleard, J.S., 2020. Contrasting patterns of isotype-1 β-tubulin allelic diversity in Haemonchus contortus and Haemonchus placei in the southern USA are consistent with a model of localised emergence of benzimidazole resistance. Vet Parasitol 286, 109240.

Chaudhry, U., Redman, E.M., Raman, M., Gilleard, J.S., 2015. Genetic evidence for the spread of a benzimidazole resistance mutation across southern India from a single origin in the parasitic nematode Haemonchus contortus. Int J Parasitol.

Cui, L., Mharakurwa, S., Ndiaye, D., Rathod, P.K., Rosenthal, P.J., 2015. Antimalarial Drug Resistance: Literature Review and Activities and Findings of the ICEMR Network. The American journal of tropical medicine and hygiene 93, 57-68.

Darghouth, M.A., Ben Miled, L., Bouattour, A., Melrose, T.R., Brown, C.G., Kilani, M., 1996. A preliminary study on the attenuation of Tunisian schizont-infected cell lines of Theileria annulata. Parasitol Res 82, 647-655.

David, K.P., Alifrangis, M., Salanti, A., Vestergaard, L.S., Ronn, A., Bygbjerg, I.B., 2003. Atovaquone/proguanil resistance in Africa: a case report. Scand J Infect Dis 35, 897-898.

de Pecoulas, P.E., Tahar, R., Ouatas, T., Mazabraud, A., Basco, L.K., 1998. Sequence variations in the Plasmodium vivax dihydrofolate reductase-thymidylate synthase gene and their relationship with pyrimethamine resistance. Mol Biochem Parasitol 92, 265-273.

Farnert, A., Lindberg, J., Gil, P., Swedberg, G., Berqvist, Y., Thapar, M.M., Lindegardh, N., Berezcky, S., Bjorkman, A., 2003. Evidence of Plasmodium falciparum malaria resistant to atovaquone and proguanil hydrochloride: case reports. Bmj 326, 628-629.

Fay, J.C., Wu, C.I., 2000. Hitchhiking under positive Darwinian selection. Genetics 155, 1405-1413.

Fivelman, Q.L., Butcher, G.A., Adagu, I.S., Warhurst, D.C., Pasvol, G., 2002. Malarone treatment failure and in vitro confirmation of resistance of Plasmodium falciparum isolate from Lagos, Nigeria. Malar J 1, 1.

Fry, M., Pudney, M., 1992. Site of action of the antimalarial hydroxynaphthoquinone, 2-[trans-4-(4'-chlorophenyl) cyclohexyl]-3-hydroxy-1,4-naphthoquinone (566C80). Biochem Pharmacol 43, 1545-1553.

Hastings, M.D., Maguire, J.D., Bangs, M.J., Zimmerman, P.A., Reeder, J.C., Baird, J.K., Sibley, C.H., 2005. Novel Plasmodium vivax dhfr alleles from the Indonesian Archipelago and Papua New Guinea: association with pyrimethamine resistance determined by a Saccharomyces cerevisiae expression system. Antimicrob Agents Chemother 49, 733-740.

Huson, D.H., Bryant, D., 2006. Application of phylogenetic networks in evolutionary studies. Mol Biol Evol 23, 254-267.

Imwong, M., Pukrittayakamee, S., Renia, L., Letourneur, F., Charlieu, J.P., Leartsakulpanich, U., Looareesuwan, S., White, N.J., Snounou, G., 2003. Novel point mutations in the dihydrofolate reductase gene of Plasmodium vivax: evidence for sequential selection by drug pressure. Antimicrob Agents Chemother 47, 1514-1521.

Jabbar, A., Abbas, T., Sandhu, Z.U., Saddiqi, H.A., Qamar, M.F., Gasser, R.B., 2015. Tick-borne diseases of bovines in Pakistan: major scope for future research and improved control. Parasites & vectors 8, 283.

Katzer, F., Carrington, M., Knight, P., Williamson, S., Tait, A., Morrison, I.W., Hall, R., 1994. Polymorphism of SPAG-1, a candidate antigen for inclusion in a sub-unit vaccine against Theileria annulata. Mol Biochem Parasitol 67, 1-10.

Kaur, S., Prajapati, S.K., Kalyanaraman, K., Mohmmed, A., Joshi, H., Chauhan, V.S., 2006. Plasmodium vivax dihydrofolate reductase point mutations from the Indian subcontinent. Acta Trop 97, 174-180.

Kessl, J.J., Ha, K.H., Merritt, A.K., Lange, B.B., Hill, P., Meunier, B., Meshnick, S.R., Trumpower, B.L., 2005. Cytochrome b mutations that modify the ubiquinol-binding pocket of the cytochrome bc1 complex and confer anti-malarial drug resistance in Saccharomyces cerevisiae. J Biol Chem 280, 17142-17148.

Kessl, J.J., Ha, K.H., Merritt, A.K., Meshnick, S.R., Trumpower, B.L., 2006. Molecular basis of Toxoplasma gondii atovaquone resistance modeled in Saccharomyces cerevisiae. Mol Biochem Parasitol 146, 255-258.

Kessl, J.J., Meshnick, S.R., Trumpower, B.L., 2007. Modeling the molecular basis of atovaquone resistance in parasites and pathogenic fungi. Trends Parasitol 23, 494-501.

Korsinczky, M., Chen, N., Kotecka, B., Saul, A., Rieckmann, K., Cheng, Q., 2000. Mutations in Plasmodium falciparum cytochrome b that are associated with atovaquone resistance are located at a putative drug-binding site. Antimicrobial Agents and Chemotherapy 44, 2100-2108.

Kozich, J.J., Westcott, S.L., Baxter, N.T., Highlander, S.K., Schloss, P.D., 2013. Development of a dual-index sequencing strategy and curation pipeline for analyzing amplicon sequence data on the MiSeq Illumina sequencing platform. Appl. Environ. Microbiol. 79, 5112-5120.

Kuesap, J., Rungsrihirunrat, K., Thongdee, P., Ruangweerayut, R., Na-Bangchang, K., 2011. Change in mutation patterns of Plasmodium vivax dihydrofolate reductase (Pvdhfr) and dihydropteroate synthase (Pvdhps) in P. vivax isolates from malaria endemic areas of Thailand. Mem Inst Oswaldo Cruz 1, 130-133.

Librado, P., Rozas, J., 2009. DnaSP v5: a software for comprehensive analysis of DNA polymorphism data. Bioinformatics 25, 1451-1452.

Lu, F., Wang, B., Cao, J., Sattabongkot, J., Zhou, H., Zhu, G., Kim, K., Gao, Q., Han, E.T., 2012. Prevalence of drug resistance-associated gene mutations in Plasmodium vivax in Central China. Korean J Parasitol 50, 379-384.

Marsolier, J., Perichon, M., DeBarry, J.D., Villoutreix, B.O., Chluba, J., Lopez, T., Garrido, C., Zhou, X.Z., Lu, K.P., Fritsch, L., Ait-Si-Ali, S., Mhadhbi, M., Medjkane, S., Weitzman, J.B., 2015.

Theileria parasites secrete a prolyl isomerase to maintain host leukocyte transformation. Nature 520, 378-382.

Mäser, P., Sütterlin, C., Kralli, A., Kaminsky, R., 1999. A nucleoside transporter from Trypanosoma brucei involved in drug resistance. Science 285, 242-244.

Matovu, E., Geiser, F., Schneider, V., Mäser, P., Enyaru, J.C., Kaminsky, R., Gallati, S., Seebeck, T., 2001. Genetic variants of the TbAT1 adenosine transporter from African trypanosomes in relapse infections following melarsoprol therapy. Molecular and biochemical parasitology 117, 73-81.

McFadden, D.C., Tomavo, S., Berry, E.A., Boothroyd, J.C., 2000. Characterization of cytochrome b from Toxoplasma gondii and Q(o) domain mutations as a mechanism of atovaquone-resistance. Mol Biochem Parasitol 108, 1-12.

McHardy, N., Hudson, A.T., Morgan, D.W., Rae, D.G., Dolan, T.T., 1983. Activity of 10 naphthoquinones, including parvaquone (993C) and menoctone, in cattle artificially infected with Theileria parva. Research in veterinary science 35, 347-352.

McHardy, N., Morgan, D.W., 1985. Treatment of Theileria annulata infection in calves with parvaquone. Research in veterinary science 39, 1-4.

McHardy, N., Wekesa, L.S., Hudson, A.T., Randall, A.W., 1985. Antitheilerial activity of BW720C (buparvaquone): a comparison with parvaquone. Research in veterinary science 39, 29-33.

Mhadhbi, M., Chaouch, M., Ajroud, K., Darghouth, M.A., BenAbderrazak, S., 2015. Sequence Polymorphism of Cytochrome b Gene in Theileria annulata Tunisian Isolates and Its Association with Buparvaquone Treatment Failure. PLoS One 10.

Mhadhbi, M., Naouach, A., Boumiza, A., Chaabani, M.F., BenAbderazzak, S., Darghouth, M.A., 2010. In vivo evidence for the resistance of Theileria annulata to buparvaquone. Vet Parasitol 169, 241-247.

Mint Lekweiry, K., Ould Mohamed Salem Boukhary, A., Gaillard, T., Wurtz, N., Bogreau, H., Hafid, J.E., Trape, J.F., Bouchiba, H., Ould Ahmedou Salem, M.S., Pradines, B., Rogier, C., Basco, L.K., Briolant, S., 2012. Molecular surveillance of drug-resistant Plasmodium vivax using pvdhfr, pvdhps and pvmdr1 markers in Nouakchott, Mauritania. J Antimicrob Chemother 67, 367-374.

Muraguri, G.R., Ngumi, P.N., Wesonga, D., Ndungu, S.G., Wanjohi, J.M., Bang, K., Fox, A., Dunne, J., McHardy, N., 2006. Clinical efficacy and plasma concentrations of two formulations of buparvaquone in cattle infected with East Coast fever (Theileria parva infection). Res Vet Sci 81, 119-126.

Musset, L., Bouchaud, O., Matheron, S., Massias, L., Le Bras, J., 2006. Clinical atovaquone-proguanil resistance of Plasmodium falciparum associated with cytochrome b codon 268 mutations. Microbes Infect 8, 2599-2604.

Nene, V., Kiara, H., Lacasta, A., Pelle, R., Svitek, N., Steinaa, L., 2016. The biology of Theileria parva and control of East Coast fever - Current status and future trends. Ticks Tick Borne Dis 7, 549-564.

Posada, D., 2008. jModelTest: phylogenetic model averaging. Molecular biology and evolution 25, 1253-1256.

Ranjitkar, S., Schousboe, M.L., Thomsen, T.T., Adhikari, M., Kapel, C.M., Bygbjerg, I.C., Alifrangis, M., 2011. Prevalence of molecular markers of anti-malarial drug resistance in Plasmodium vivax and Plasmodium falciparum in two districts of Nepal. Malar J 10, 75.

Sargison, N.D., MacLeay, M., Morrison, A.A., Bartley, D.J., Evans, M., Chaudhry, U., 2019. Development of amplicon sequencing for the analysis of benzimidazole resistance allele frequencies in field populations of gastrointestinal nematodes. International journal for parasitology. Drugs and drug resistance 10, 92-100.

Schloss, P.D., Westcott, S.L., Ryabin, T., Hall, J.R., Hartmann, M., Hollister, E.B., Lesniewski, R.A., Oakley, B.B., Parks, D.H., Robinson, C.J., 2009. Introducing mothur: open-source, platform-independent, community-supported software for describing and comparing microbial communities. Appl. Environ. Microbiol. 75, 7537-7541.

Schunk, M., Kumma, W.P., Miranda, I.B., Osman, M.E., Roewer, S., Alano, A., Loscher, T., Bienzle, U., Mockenhaupt, F.P., 2006. High prevalence of drug-resistance mutations in Plasmodium falciparum and Plasmodium vivax in southern Ethiopia. Malar J 5, 1475-2875.

Schwartz, E., Bujanover, S., Kain, K.C., 2003. Genetic confirmation of atovaquone-proguanil-resistant Plasmodium falciparum malaria acquired by a nonimmune traveler to East Africa. Clin Infect Dis 37, 450-451.

Schwobel, B., Alifrangis, M., Salanti, A., Jelinek, T., 2003. Different mutation patterns of atovaquone resistance to Plasmodium falciparum in vitro and in vivo: rapid detection of codon 268 polymorphisms in the cytochrome b as potential in vivo resistance marker. Malar J 2, 5.

Sharifiyazdi, H., Namazi, F., Oryan, A., Shahriari, R., Razavi, M., 2012. Point mutations in the Theileria annulata cytochrome b gene is associated with buparvaquone treatment failure. Vet Parasitol 187, 431-435.

Shaukat, A., Ali, Q., Connelley, T., Khan, M.A.U., Saleem, M.A., Evans, M., Rashid, I., Sargison, N.D., Chaudhry, U., 2019. Selective sweep and phylogenetic models for the emergence and spread of pyrimethamine resistance mutations in Plasmodium vivax. Infect Genet Evol 68, 221-230.

Shaukat, A., Ali, Q., Raud, L., Wahab, A., Khan, T.A., Rashid, I., Rashid, M., Hussain, M., Saleem, M.A., Sargison, N.D., Chaudhry, U., 2021. Phylogenetic analysis suggests single and multiple origins of dihydrofolate reductase mutations in Plasmodium vivax. Acta Trop 215, 105821.

Siregar, J.E., Syafruddin, D., Matsuoka, H., Kita, K., Marzuki, S., 2008. Mutation underlying resistance of Plasmodium berghei to atovaquone in the quinone binding domain 2 (Qo(2)) of the cytochrome b gene. Parasitol Int 57, 229-232.

Song, Z., Clain, J., Iorga, B.I., Yi, Z., Fisher, N., Meunier, B., 2015. Saccharomyces cerevisiae-based mutational analysis of the bc1 complex Qo site residue 279 to study the trade-off between atovaquone resistance and function. Antimicrobial agents and chemotherapy 59, 4053-4058.

Srivastava, I.K., Morrisey, J.M., Darrouzet, E., Daldal, F., Vaidya, A.B., 1999. Resistance mutations reveal the atovaquone-binding domain of cytochrome b in malaria parasites. Mol Microbiol 33, 704-711.

Syafruddin, D., Siregar, J.E., Marzuki, S., 1999. Mutations in the cytochrome b gene of Plasmodium berghei conferring resistance to atovaquone. Mol Biochem Parasitol 104, 185-194.

Tajima, F., 1989. Statistical method for testing the neutral mutation hypothesis by DNA polymorphism. Genetics 123, 585-595.

Figure Legend

Figure 1: Relative allele frequencies of cytochrome b resistance-associated mutations in 75 buffalo-derived and 119 cattle-derived *T. annulata* isolates collected from endemic regions of Pakistan. Each isolate shows the relative frequency of the resistant versus susceptible SNP based on allele quantification by deep amplicon sequencing (Supplementary Table S3). The susceptible SNP frequency - S129 (AG), P253 (CCT) and L262 (TTA) - is shown in red and resistance-associated SNP frequency - 129G (GGC), 253S (TCT), 262S (TCA) and 129G (GGC)/ 253S (TCT) - is shown in light green, dark green, blue and pink.

Figure 2: Twenty-two buffalo-derived (2A) and 61 cattle-derived (2B) haplotypes of the cytochrome b locus were generated using the FaBox 1.5 tool (birc.au.dk). The 9/22 buffalo-derived and 21/61 cattle-derived resistance haplotypes (BHA and CHA) are represented by a different colour for the individual isolates (CY). Susceptible haplotypes are not indicated in the figure but are shown in Table 3. The haplotype distribution and the frequency based on the sequence reads generated per *T. annulata* isolates are shown in the insert table.

Figure 3: A split tree of 22 buffalo and 61 cattle-derived haplotypes of cytochrome b locus was generated in SplitsTrees4 software (Huson and Bryant, 2006). The pie chart circles represent the different haplotypes and the size of each circle is proportional to the number of sequence reads and frequency generated in that haplotype as indicated in the inserted table. **(A)** The mutation carried buffalo-derived *T. annulata* haplotypes is shaded as follows: thirteen susceptible haplotypes are shown by grey shading; six 129G (GGC) resistant haplotypes are shaded black; one 129G (GGC)/ 253S (TCT) double mutant resistant haplotype is shown by black line shading; and two 253S (TCT) resistant haplotypes are shown by white shading. **(B)** The mutation-carrying cattle-derived *T. annulata* haplotypes are shaded as follows: forty susceptible haplotypes are shown by grey shading; twelve 129G (GGC) resistant haplotypes are shown by black shading; three 262S (TCA) resistant haplotypes are shown by black line shading, and six 253S (TCT) resistant haplotypes are shown by white shading.

Figure 4: A network tree of 22 buffalo-derived and 61 cattle-derived haplotypes of cytochrome b locus was generated in Network 4.6.1 software (Fluxus Technology Ltd). The size of each pie chart circle representing the haplotype was proportional to the number of sequences generated from different isolates. The colours in the pie chart circles replicate the haplotype frequency and their distribution as indicated in the inserted table. **(A)** The buffalo-derived *T. annulata* carried thirteen susceptible haplotypes, six 129G (GGC) resistant haplotypes, one 129G (GGC)/ 253S (TCT) double mutant resistant haplotype and two 253S (TCT) resistant haplotypes. The mutation-carrying buffalo derived *T. annulata* haplotypes in different livestock farms are shown in the inserted map. **(B)** The cattle-derived *T. annulata* carried forty susceptible haplotypes, twelve 129G (GGC) resistant haplotypes, three 262S (TCA) resistant haplotypes and six 253S (TCT) resistant haplotypes. The mutation-carrying cattle-derived *T. annulata* haplotypes in different livestock farms are shown in the inserted map.

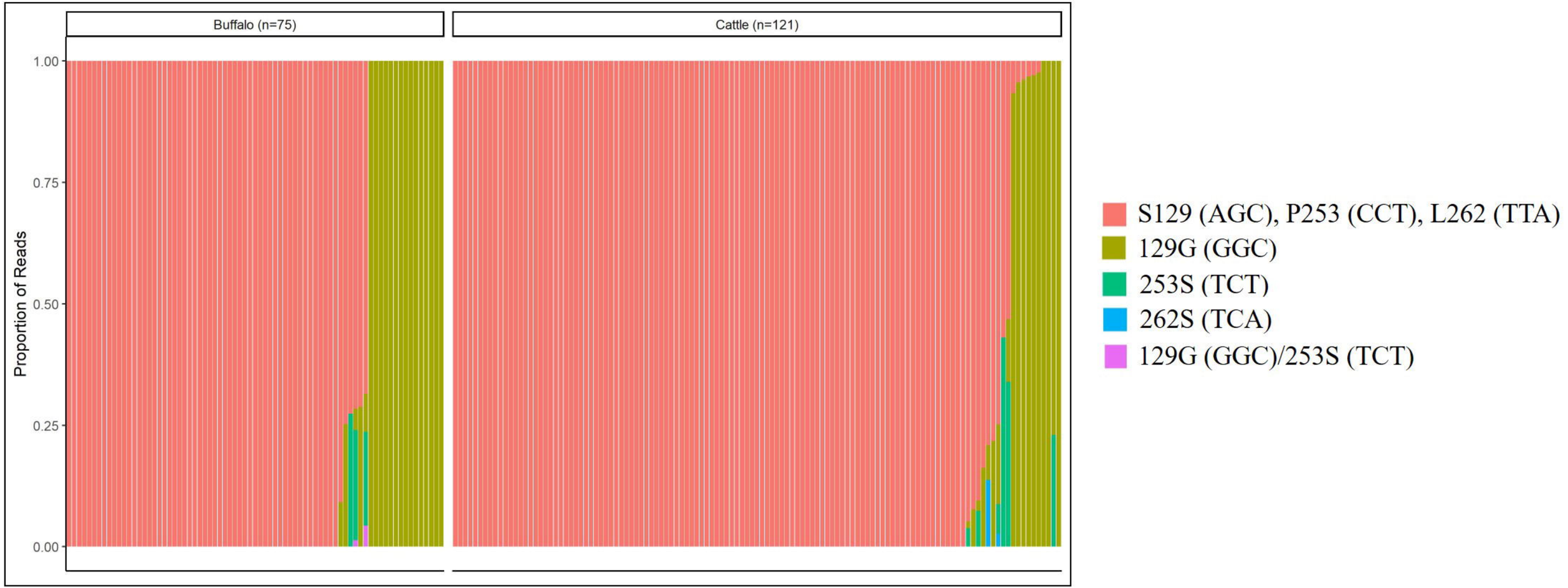
Buffalo (n=75)
Cattle (n=121)
Proportion of Reads
1.00
0.75
0.50
0.25
0.00
S129 (AGC), P253 (CCT), L262 (TTA)
129G (GGC)
253S (TCT)
262S (TCA)
129G (GGC)/253S (TCT)

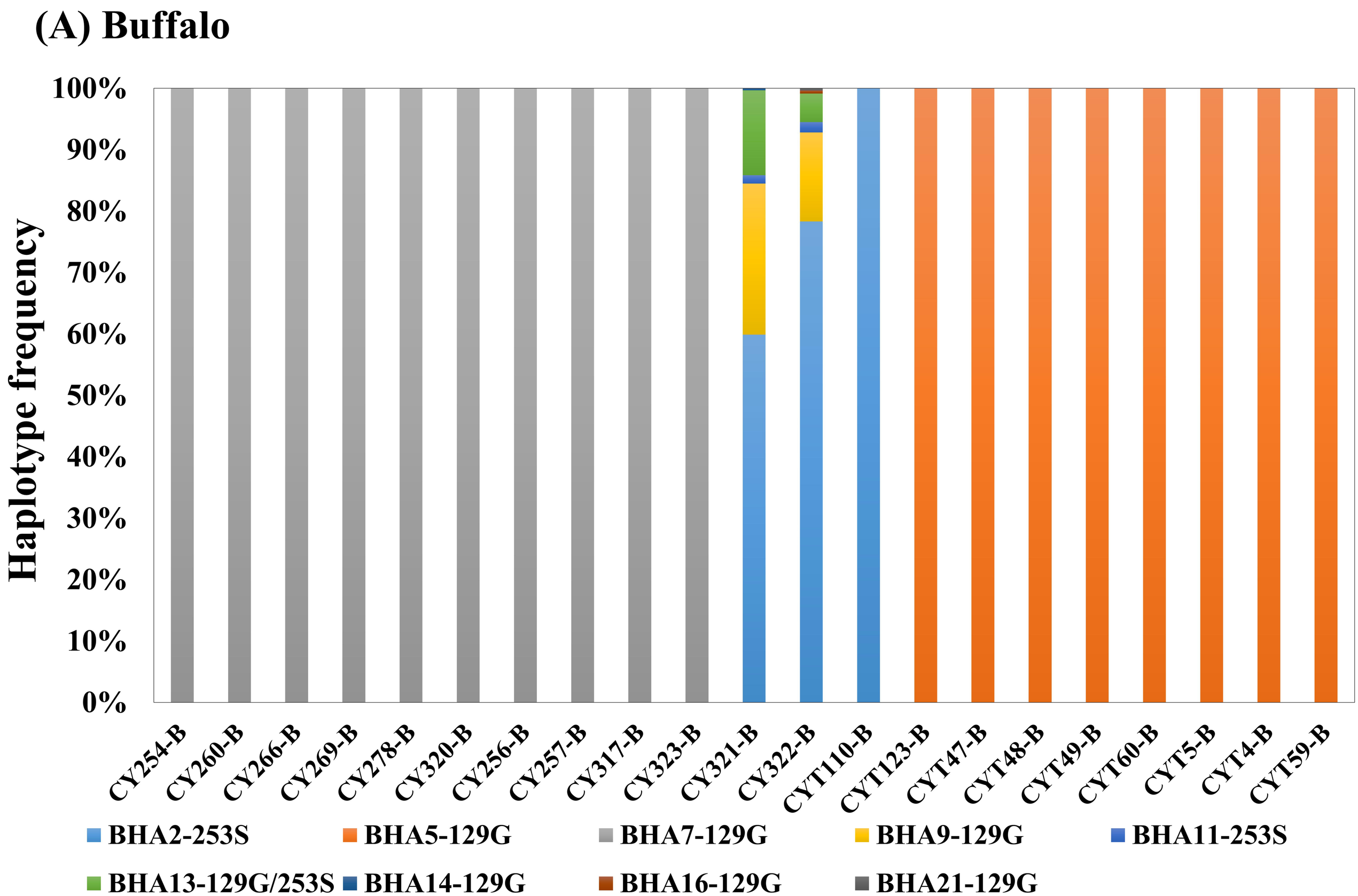

Field isolates	BHA2-253S	BHA5-129G	BHA7-129G	BHA9-129G	BHA11-253S	BHA13-129G/253S	BHA14-129G	BHA16-129G	BHA21-129G
CY254-B			100						
CY260-B			100						
CY266-B			100						
CY269-B			100						
CY278-B			100						
CY320-B			100						
CY256-B			100						
CY257-B			100						
CY317-B			100						
CY323-B			100						
CY321-B	59.9			24.5	1.3	13.8	0.3		
CY322-B	78.3			14.4	1.6	4.6	0	0.5	0.3
CY110-B	100								
CY123-B		100							
CY47-B		100							
CY48-B		100							
CY49-B		100							
CY60-B		100							
CY5-B		100							
CY4-B		100							
CY59-B		100							

(B) Cattle

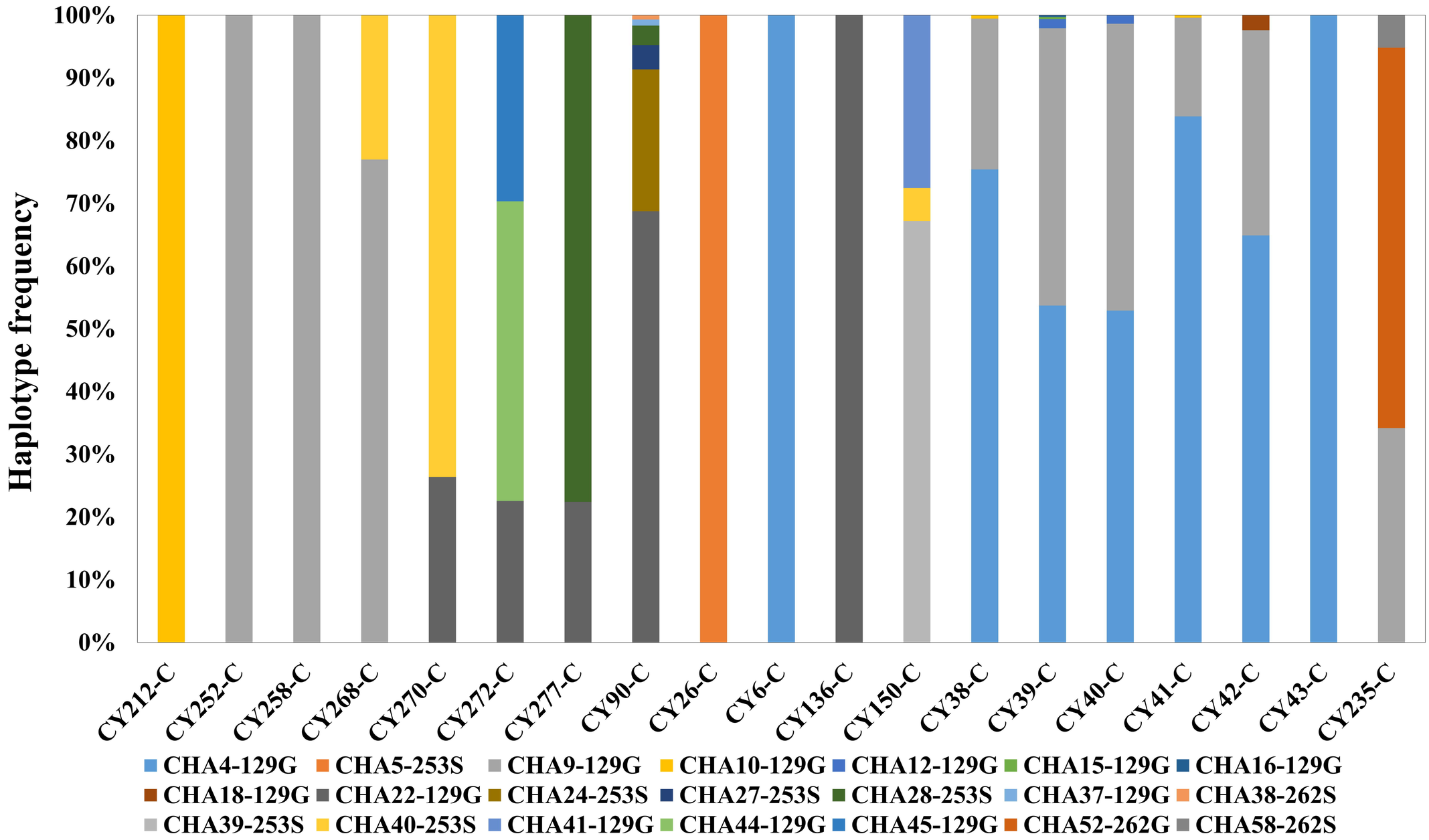

Field isolates	CHA4-129G	CHA5-253S	CHA9-129G	CHA10-129G	CHA12-129G	CHA15-129G	CHA16-129G	CHA18-129G	CHA22-129G	CHA24-253S	CHA27-253S	CHA28-253S	CHA37-129G	CHA38-262S	CHA39-253S	CHA40-253S	CHA41-129G	CHA44-129G	CHA45-129G	CHA52-262G	CHA58-262S
CY212-C				100																	
CY252-C			100																		
CY258-C			100																		
CY268-C			77													23.0					
CY270-C									26.4							73.6					
CY272-C									22.6									47.8	29.7		
CY277-C									22.4			77.6									
CY90-C									68.8	22.6	3.9	3.1	1.0	0.7							
CY26-C		100																			
CY6-C	100																				
CY136-C									100												
CY150-C															67.2	5.2	27.6				
CY38-C	75		24.1	0.5																	
CY39-C	54		44.2		1.5	0.3	0.3														
CY40-C	53		45.7		1.4																
CY41-C	84		15.7	0.4																	
CY42-C	65		32.7					2.4													
CY43-C	100																				
CY235-C			34.2																	60.6	5.2

(A) Buffalo

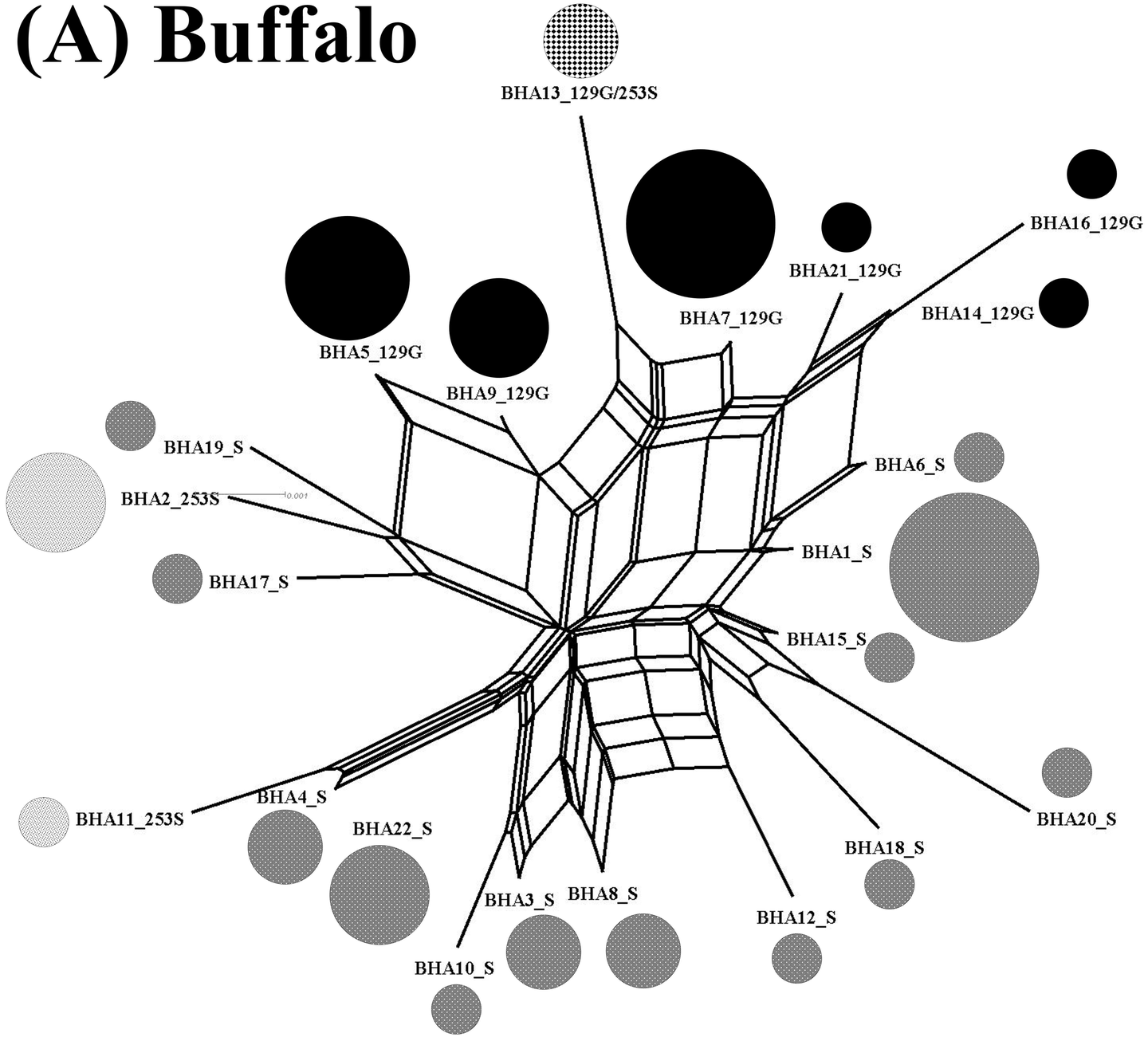

Susceptible and resistant haplotype	Total no of Illumina MiSeq reads	Total no of Illumina MiSeq reads (%)
BHA7-129G	192096	6
BHA1-S	145769	6
BHA5-129G	84673	5
BHA2-253S	32480	4
BHA22-S	16127	4
BHA9-129G	6096	4
BHA3-S	3469	3
BHA4-S	3171	3
BHA10-S	3396	3
BHA13-129G/253S	2409	3
BHA8-S	1887	3
BHA6-S	998	2
BHA11-253S	594	1.5
BHA12-S	452	1.5
BHA15-S	246	1.5
BHA16-129G	145	1.5
BHA17-S	147	1.5
BHA18-S	133	1.5
BHA19-S	129	1.5
BHA20-S	109	1.5
BHA21-129G	104	1.5
BHA14-129G	24	1.5

(B) Cattle

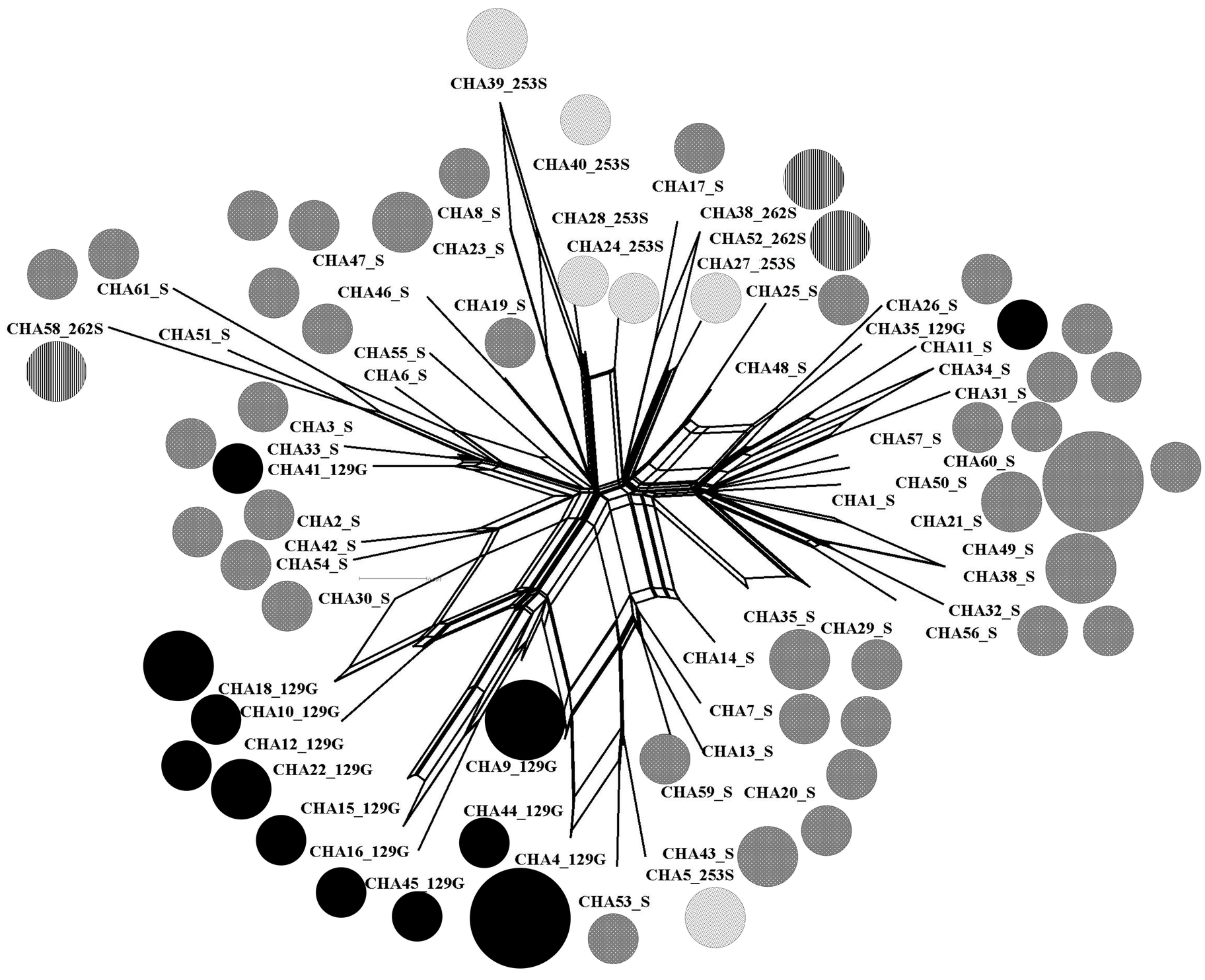

Susceptible and resistant haplotype	Total no of Illumina MiSeq reads	Total no of Illumina MiSeq reads (%)
CHA1-S	202028	27.17
CHA4-129G	181194	24.37
CHA9-129G	95262	12.81
CHA21-S	40517	5.45
CHA10-129G	38291	5.15
CHA50-S	26595	3.58
CHA22-129G	19249	2.59
CHA43-S	14901	2.00
CHA35-S	12980	1.75
CHA5-253S	12346	1.66
CHA51-S	11298	1.52
CHA31-S	10559	1.42
CHA23-S	9189	1.24
CHA39-253S	8825	1.19
CHA52-262G	7664	1.03
CHA40-253S	4885	0.66
CHA28-253S	4681	0.63
CHA53-S	3656	0.49
CHA41-129G	3621	0.49
CHA24-253S	3472	0.47
CHA11-S	2911	0.39
CHA7-S	2519	0.34
CHA8-S	2429	0.33
CHA44-129G	2421	0.33
CHA54-S	1904	0.26
CHA55-S	1627	0.22
CHA19-S	1534	0.21
CHA45-129G	1504	0.20
CHA18-129G	1381	0.19
CHA2-S	1154	0.16
CHA56-S	1041	0.14
CHA12-129G	1018	0.14
CHA3-S	1006	0.14
CHA57-S	979	0.13
CHA25-S	964	0.13
CHA42-S	782	0.11
CHA26-S	746	0.10
CHA58-262S	655	0.09
CHA27-253S	594	0.08
CHA47-S	574	0.08
CHA20-S	539	0.07
CHA59-S	367	0.05
CHA29-S	347	0.05
CHA60-S	343	0.05
CHA30-S	327	0.04
CHA48-S	274	0.04
CHA32-S	210	0.03
CHA46-S	201	0.03
CHA13-S	188	0.03
CHA49-S	188	0.03
CHA33-S	185	0.02
CHA34-S	185	0.02
CHA36-S	159	0.02
CHA37-129G	147	0.02
CHA6-S	146	0.02
CHA61-S	139	0.02
CHA14-S	135	0.02
CHA15-129G	133	0.02
CHA17-S	132	0.02
CHA16-129G	125	0.02
CHA38-262S	108	0.01

(A) Buffalo

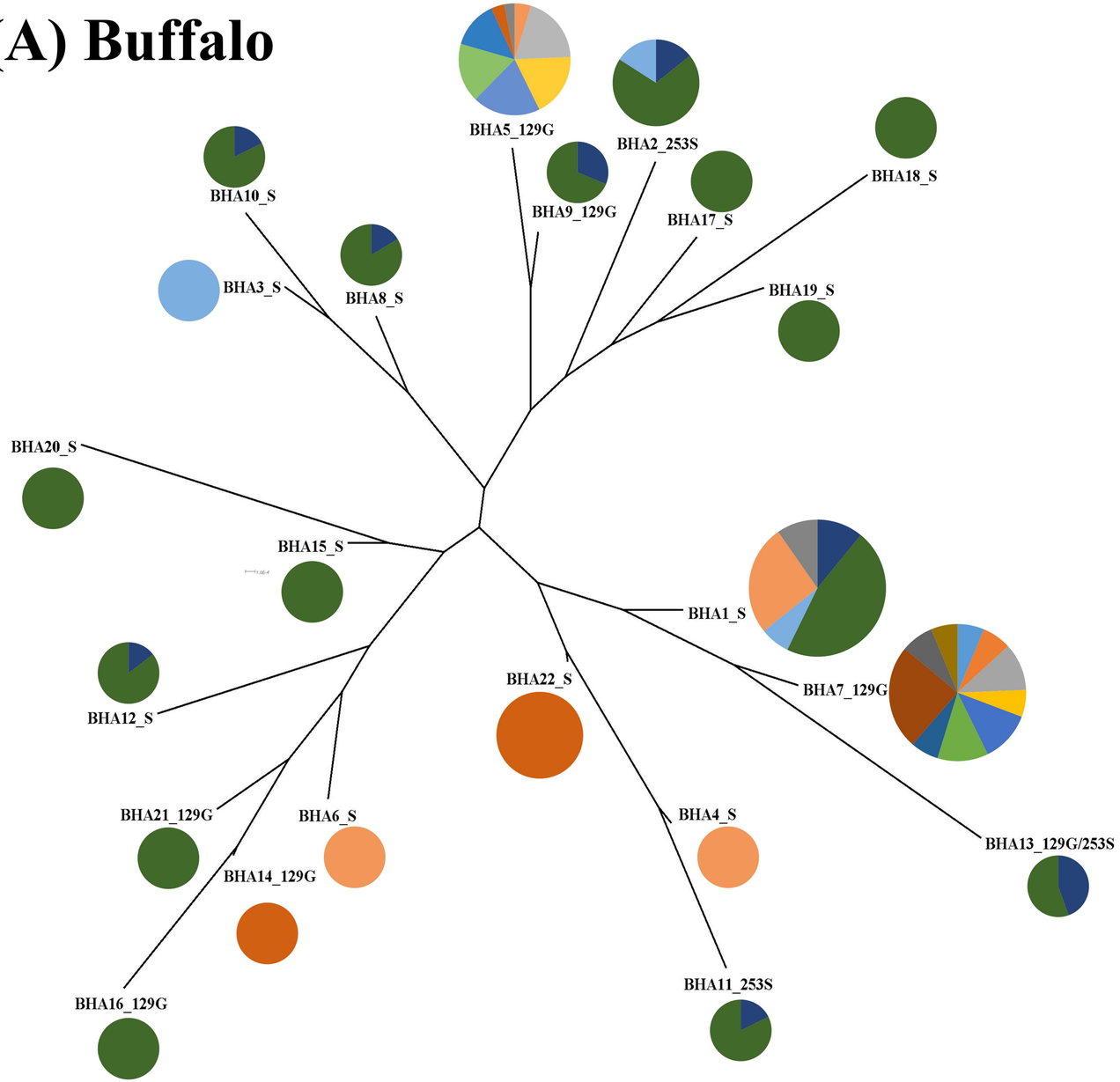

Susceptible and resistant haplotypes	Isolates (%)
BHA1-S	CY321-B (10.8), CY322-B(46.3), CYT110-B(7), CYT123-B(26)
BHA2-253S	CY321-B (14.2), CY322-B(69.8), CYT110-B(15.9)
BHA3-S	CYT110-B(100)
BHA4-S	CYT123-B(100)
BHA5-129G	CYT123-B(5), CYT47-B(20.8), CYT48-B(19.5), CYT49-B(14.5), CYT60-B(18.2), CYT5-B(14.5), CYT4-B(4), CYT59-B(3.1)
BHA6-S	CYT123-B(100)
BHA7-129G	CY254-B(6.3),CY260-B(6.9), CY266-B(11.3), CY269-B(6.4), CY278-B(10.9), CY320-B(12.1), CY256-B(6.7), CY257-B(24.9), CY317-B(7.8), CY323-B(6.3)
BHA8-S	CY321-B(16.4), CY322-B(83.5)
BHA9-129G	CY321-B(31.2), CY322-B(68.7)
BHA10-S	CY321-B(17.6), CY322-B(82.3)
BHA11-253S	CY321-B(17.6), CY322-B(82.3)
BHA12-S	CY321-B(14.6), CY322-B(85.3)
BHA13-129G/253S	CY321-B(44.4), CY322-B(55.5)
BHA14-129G	CY321-B(100)
BHA15-S	CY322-B(100)
BHA16-129G	CY322-B(100)
BHA17-S	CY322-B(100)
BHA18-S	CY322-B(100)
BHA19-S	CY322-B(100)
BHA20-S	CY322-B(100)
BHA21-129G	CY322-B(100)
BHA22-S	CYT4-B(100)

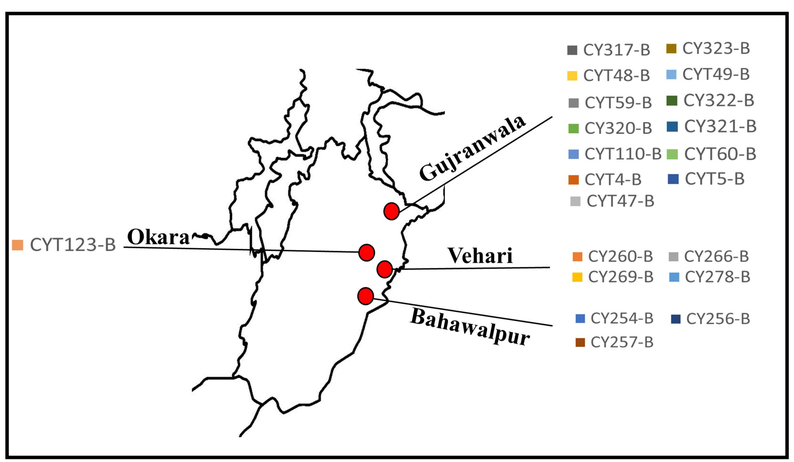

(B) Cattle

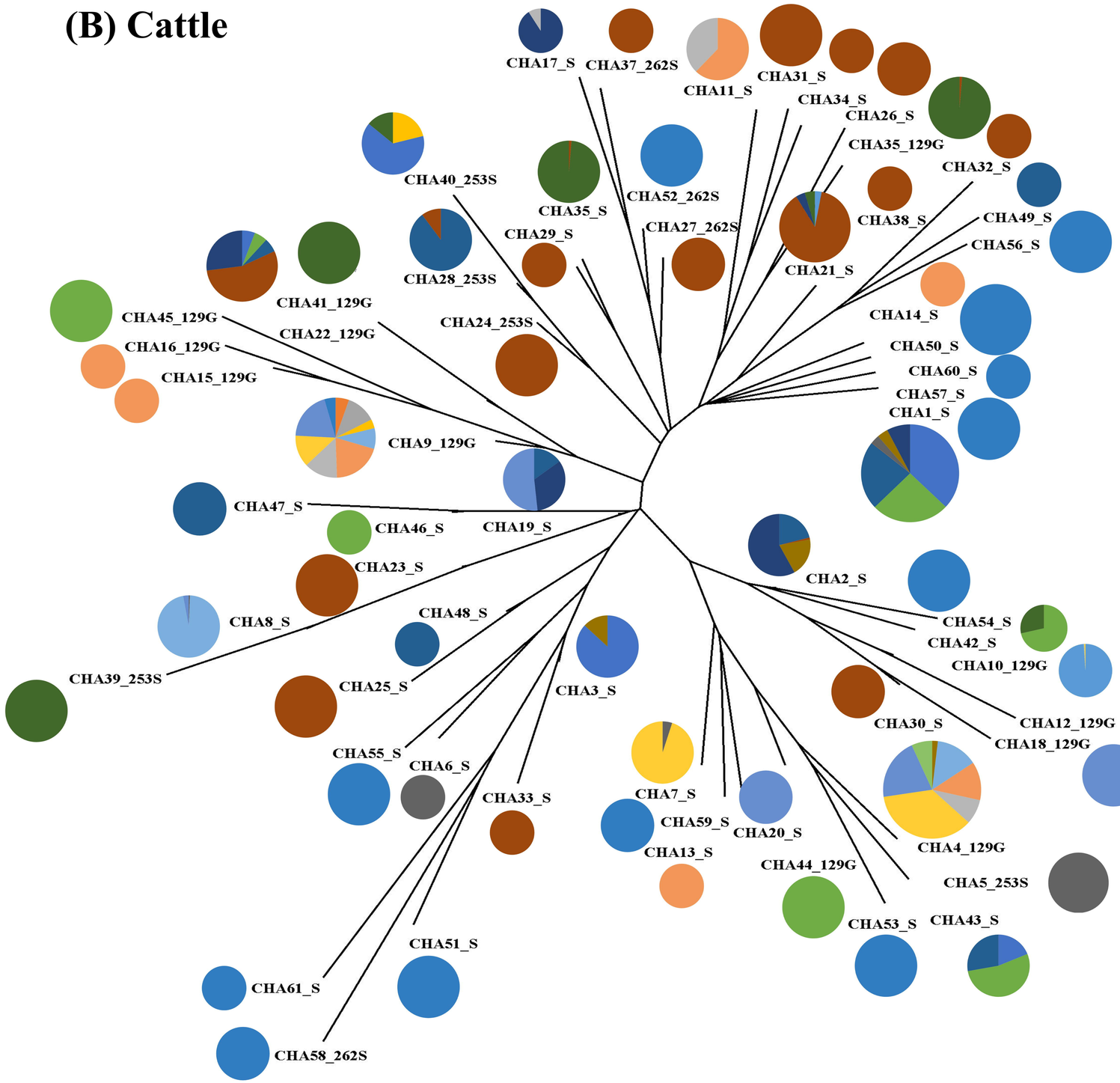

Susceptible and resistant haplotypes	Isolates (%)
CHA1-S	CY270-C(37), CY272-C (25.7), CY277-C (22.7), CY90-C (0.1), CY26-C (2.9), CY6-C (3.5), CY136-C (7.7)
CHA2-S	CY277-C (21.1), CY90-C (1), CY6-C (19.8), CY136-C (58.1)
CHA3-S	CY270-C (86.9), CY6-C (13.1)
CHA4-129G	CY6-C (1.9), CY38-C (13.8), CY39-C (8.2), CY40-C (36), CY41-C (36), CY42-C (20.5), CY43-C (6.8)
CHA5-253S	CY6-C (100)
CHA6-S	CY6-C (100)
CHA7-S	CY26-C (5), CY41-C (95)
CHA8-S	CY26-C (0.7), CY38-C (96.5), CY42-C (2.9)
CHA9-129G	CY252-C (5.4), CY258-C (12), CY268-C (3.6), CY38-C (8.4), CY39-C (19.9), CY40-C (13.5), CY41-C (12.9), CY42-C (19.6), CY235-C (4.5)
CHA10-129G	CY212-C (98.7), CY38-C (0.4), CY41-C (0.8)
CHA11-S	CY39-C (62.2), CY40-C (37.8)
CHA12-129G	CY39-C (62.7), CY40-C (37.3)
CHA13-S	CY39-C (100)
CHA14-S	CY39-C (100)
CHA15-129G	CY39-C (100)
CHA16-129G	CY39-C (100)
CHA17-S	CY136-C (90.9), CY40-C (9.1)
CHA18-129G	CY42-C (100)
CHA19-S	CY277-C (15), CY136-C (33.2), CY51.7)-C
CHA20-S	CY42-C (100)
CHA21-S	CY212-C (3), CY90-C (88.1), CY136-C (4.2), CY150-C (4.6)
CHA22-129G	CY270-C (5.8), CY272-C (5.9), CY277-C (6.3), CY90-C (54.8), CY136-C (27)
CHA23-S	CY90-C (100)
CHA24-253S	CY90-C (100)
CHA25-S	CY90-C (100)
CHA26-S	CY90-C (100)
CHA27-253S	CY90-C (100)
CHA28-253S	CY277-C (89.8), CY90-C (10.1)
CHA29-S	CY90-C (100)
CHA30-S	CY90-C (100)
CHA31-S	CY90-C (100)
CHA32-S	CY90-C (100)
CHA33-S	CY90-C (100)
CHA34-S	CY90-C (100)
CHA35-S	CY90-C (1.3), CY150-C (98.7)
CHA36-S	CY90-C (100)
CHA37-129G	CY90-C (100)
CHA38-262S	CY90-C (100)
CHA39-253S	CY150-C (100)
CHA40-253S	CY268-C (21.1), CY270-C (64.76), CY150-C (14.1)
CHA41-129G	CY150-C (100)
CHA42-S	CY272-C (71.4), CY150-C (28.5)
CHA43-S	CY270-C (18.8), CY272-C (53.3), CY77-C (27.7)
CHA44-129G	CY272-C (100)
CHA45-129G	CY272-C (100)
CHA46-S	CY272-C (100)
CHA47-S	CY277-C (100)
CHA48-S	CY277-C (100)
CHA49-S	CY277-C (100)
CHA50-S	CY235-C (100)
CHA51-S	CY235-C (100)
CHA52-262G	CY235-C (100)
CHA53-S	CY235-C (100)
CHA54-S	CY235-C (100)
CHA55-S	CY235-C (100)
CHA56-S	CY235-C (100)
CHA57-S	CY235-C (100)
CHA58-262S	CY235-C (100)
CHA59-S	CY235-C (100)
CHA60-S	CY235-C (100)
CHA61-S	CY235-C (100)

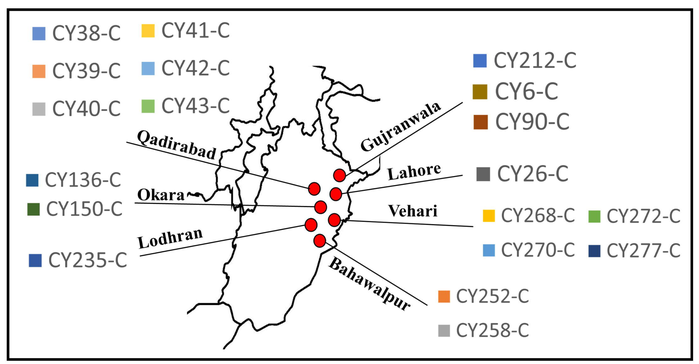

Table 1. Cytochrome b mutations identified in buparvaquone susceptible *T. annulata* isolates collected from an endemic region of Turkey, India, Tunisia, and Morocco and resistant *T. annulata* isolates collected from an endemic region of Tunisia. Comparison shows the buparvaquone susceptible (674, Battan C, Battan P4, Chargui P5, Jed4, Jes4P10, TA-ANK, TA-BUT, TA-HAS, TA-MARR) and resistant isolates (739, 881III, 5911, 8307, BC2T, ST2/13, ST2/19). Nonsynonymous mutations at positions S129G (AGC/GGC), P253S (CCT/TCT) and L262S (TTA/TCA) in the binding pockets Q_{01} and Q_{02} of the cytochrome b locus differ between susceptible and resistant *T. annulata* isolates.

		Q01 (130-148)											**Q02 (244-266)**	
	Nucleotide	**385 (AGC/GGC)**	398 (GCT/GTT)	403 (GTC/TTC)	406 (ATA/CTA)	413 (GGT/GTT)	418 (TTG/TTT)	420 (TTG/TTT	423 (AAA/AAC)	427 (GGA/GTA)	431 (GGA/GTA)	436 (ACT/GCT)	**757 (CCT/TCT)**	**785 (TTA/TCA)**
	Codon	**S129G**	A133V	V135F	I136L	G138V	L139F	L140F	K141N	F143L	G144V	T146A	**P253S**	**L262S**
Susceptible isolates	674	**S**	A	V	I	G/V	L/F	L/F	K	F	G/V	T	**P**	**L**
	Battan C	**S**	A	V/F	I	G/V	L/F	L/F	K/N	F/L	G/V	T	**P**	**L**
	Battan P4	**S**	A/V	V/F	I/L	G/V	L/F	L/F	K/N	F	G/V	T	**P**	**L**
	Chargui P5	**S**	A/V	V/F	I/L	G	L/F	L/F	K/N	F/L	G/V	T	**P**	**L**
	Jed4	**S**	A	V	I	G	L	L/F	K	F/L	G/V	T	**P**	**L**
	Jed4P10	**S**	A	V/F	I/L	G/V	L/F	L/F	K	F/L	G/V	T	**P**	**L**
	TA-ANK	**S**	A	V	I	G	L	L	K	F	G	T/A	**P**	**L**
	TA-BUT	**S**	A	V	I	G	L	L	K	F	G	T/A	**P**	**L**
	TA-HAS	**S**	A	V	I	G	L	L	K	F	G	T	**P**	**L**
	TA-MARR	**S**	A	V	I	G	L	L	K	F	G	T/A	**P**	**L**
Resistant isolates	739	**S/G**	A	V/F	I	G/V	L/F	L/F	K	F	G/V	T	**P/S**	**L/S**
	881III	**S/G**	A	V	I	G/V	L	L/F	K	F	G/V	T	**P/S**	**L**
	5911	**S/G**	A	V/F	I	G	L/F	L/F	K	F	G/V	T/A	**P/S**	**L**
	8307	**S/G**	A	V/F	I	G/V	L	L/F	K	F	G/V	T	**P/S**	**L**
	BC2T	**S/G**	A	V	I	G/V	L	L/F	K	F	G/V	T	**P/S**	**L**
	ST2/13	**S**	A	V/F	I	G/V	L/F	L/F	K/N	F	G/V	T/A	**P/S**	**L/S**
	ST2/19	**S/G**	A/V	V/F	I/L	G/V	L/F	L/F	K	F	G/V	T	**P/S**	**L/S**

Table 2. Relative allele frequencies of the cytochrome b mutations in 21 buffalo-derived and 19 cattle-derived *T. annulata* resistant isolates collected from the endemic region of Pakistan. Each isolate was characterized by susceptible [S129 (AGC), P253 (CCT) and L262 (TTA)] and resistance mutations [129G (GGC), 253S (TCT), 262S (TCA) and 129G (GGC)/253S (TCT)]. The relative allele frequency of the resistant versus susceptible mutations was based on the SNPs identified using the deep amplicon sequencing method.

Field isolates	Total no of Illumina MiSeq reads	Susceptible reads	Resistance reads	Susceptible reads % [S129(AGC), P253 (CCT), L262(TTA)]	Resistant reads % [129G(GGC)]	Resistant reads % [253S(TCT)]	Resistant reads % [262S(TCA)]	Resistant reads % [129G(GGC)/253S(TCT)]	Location
Buffalo									
CY110-B	18868	13699	5169	72.6		27.3			Gujranwala
CY123-B	46438	42178	4260	90.8	9.17				Okara
CY59-B	19801	14110	5691	71.2	28.7				Gujranwala
CY49-B	12313		12313		100				Gujranwala
CY5-B	12341		12341		100				Gujranwala
CY48-B	16542		16542		100				Gujranwala
CY4-B	21578	16127	5451	74.7	25.2				Gujranwala
CY60-B	15433		15433		100				Gujranwala
CY47-B	17642		17642		100				Gujranwala
CY254-B	12256		12256		100				Bahawalpur
CY256-B	12892		12892		100				Bahawalpur
CY257-B	47942		47942		100				Bahawalpur
CY260-B	13314		13314		100				Vehari
CY266-B	21823		21823		100				Vehari
CY269-B	12378		12378		100				Vehari
CY278-B	21004		21004		100				Vehari
CY317-B	14988		14988		100				Gujranwala
CY320-B	23324		23324		100				Gujranwala
CY321-B	24581	16842	7739	68.5	7.8	19.2		4.3	Gujranwala
CY322-B	102021	73077	28944	71.6	4.3	22.7		1.3	Gujranwala
CY323-B	12175				100				Gujranwala
Cattle									
CY90-C	65051	48644	16407	74.7	16.4	6.0	2.6		Gujranwala
CY136-C	23906	18706	5200	78.2	21.7				Okara
CY150-C	28039	14904	13135	53.1	12.9	33.9			Okara
CY6-C	21001	17589	3412	83.75	16.2				Gujranwala
CY26-C	28672	16326	12346	56.9		43.0			Lahore
CY38-C	35600	2343	33257	6.5	93.4				Qadirabad
CY39-C	45065	1999	43066	4.4	95.5				Qadirabad
CY40-C	29245	1113	28132	3.8	96.1				Qadirabad
CY41-C	80153	2393	77760	2.9	97.0				Qadirabad
CY42-C	58645	1402	57243	2.3	97.6				Qadirabad
CY43-C	12398		12398		100				Qadirabad
CY277-C	57086	51667	5419	90.5	2.1	7.3			Vehari
CY272-C	65893	60825	5068	92.3	7.6				Vehari
CY235-C	60586	47949	12637	79.1	7.1		13.7		Lodhran
CY268-C	4483		4483		76.9	23.0			Vehari
CY212-C	39057	1240	37817	3.1	96.8				Gujranwala
CY252-C	5173		5173		100				Bahawalpur
CY270-C	79794	78497	4297	98.3	1.4	3.9			Vehari
CY258-C	11512		11512		100				Bahawalpur

Table 3: Haplotype diversity and signature of selection at the *T. annulata* cytochrome b locus. A total number of susceptible and resistant haplotypes from 21 buffalo-derived and 19 cattle-derived *T. annulata* isolates showed the haplotype diversity and signature of selection at the cytochrome b locus.

Field isolates	Haplotype distribution						Neutrality tests	
	Total haplotypes	Susceptible haplotypes	129G(GGC) resistance haplotype	253S(TCT) resistance haplotype	262S(TCA) resistance haplotype	129G(GGC)/253S(TCT) resistance haplotype	Fay and Wu 's (H)	Tajima (D)
Buffalo								
CY110-B	3	2		1			1.61917	1.95807
CY123-B	4	3	1				1.56652	1.95807
CY59-B	2	1	1				1.70958	2.46226
CY49-B	1		1				N/A	
CY5-B	1		1				N/A	
CY48-B	1		1				N/A	
CY4-B	2	1	1				1.55322	2.23140
CY60-B	1		1				N/A	
CY47-B	1		1				N/A	
CY254-B	1		1				N/A	
CY256-B	1		1				N/A	
CY257-B	1		1				N/A	
CY260-B	1		1				N/A	
CY266-B	1		1				N/A	
CY269-B	1		1				N/A	
CY278-B	1		1				N/A	
CY317-B	1		1				N/A	
CY320-B	1		1				N/A	
CY321-B	9	4	2	2		1	1.68770*	1.75932*
CY322-B	15	9	3	2		1	1.10119*	0.88492*
CY323-B	1		1				N/A	
Total	*22*	*13*	*6*	*2*		*1*		
Cattle								
CY90-C	20	14	2	2	2		1.02457*	-0.58541*
CY136-C	6	5	1				1.26900	0.82865
CY150-C	6	3	1	2			1.39349	0.75819
CY6-C	4	3	1					
CY26-C	5	4		1				
CY38-C	4	1	3				1.54706*	1.44162
CY39-C	8	3	5				1.74256*	2.00448*
CY40-C	5	2	3				1.69795*	1.64710
CY41-C	4	1	3				1.62083*	1.98644
CY42-C	6	3	3				1.53179*	1.28502
CY43-C	1		1				N/A	
CY277-C	9	7	1	1			1.04126	-0.29438
CY272-C	7	4	3				1.57241*	1.52030
CY235-C	13	10	1		2		1.39659	0.51934
CY268-C	2		1	1			1.67822*	2.34668
CY212-C	2	1	1					
CY252-C	1		1				N/A	
CY270-C	5	3	1	1			1.38874*	1.01660
CY258-C	1		1				N/A	
Total	*61*	*40*	*12*	*6*	*3*			

Statistically significant departure from neutrality determined with the use of simulations of the coalescent at $p<0.05$*

Supplementary Table S1. Primer sequences for Illumina MiSeq Library preparation. Tann-ForAdp/Tann-RevAdp primer sequence are underlined, N's are in bold.

Sequences (5'-3')	Primer Name
TCGTCGGCAGCGTCAGATGTGTATAAGAGACAG<u>AAGTATAGCAACTGCTTTTGTT</u>	Tann-ForAdp
TCGTCGGCAGCGTCAGATGTGTATAAGAGACAG**N**<u>AAGTATAGCAACTGCTTTTGTT</u>	Tann-ForAdp1N
TCGTCGGCAGCGTCAGATGTGTATAAGAGACAG**NN**<u>AAGTATAGCAACTGCTTTTGTT</u>	Tann-ForAdp2N
TCGTCGGCAGCGTCAGATGTGTATAAGAGACAG**NNN**<u>AAGTATAGCAACTGCTTTTGTT</u>	Tann-ForRdp3N
GTCTCGTGGGCTCGGAGATGTGTATAAGAGACAG<u>TCCTGCCATTGCCAAAAGTC</u>	Tann-RevAdp
GTCTCGTGGGCTCGGAGATGTGTATAAGAGACAG**N**<u>TCCTGCCATTGCCAAAAGTC</u>	Tann-RevAdp1N
GTCTCGTGGGCTCGGAGATGTGTATAAGAGACAG**NN**<u>TCCTGCCATTGCCAAAAGTC</u>	Tann-RevAdp2N
GTCTCGTGGGCTCGGAGATGTGTATAAGAGACAG**NNN**<u>TCCTGCCATTGCCAAAAGTC</u>	Tann-Revdp3N

Supplementary Table S2. Sequences for forward and reverse barcoded primers (Nextera XT Index Kit v2). Index sequences are highlighted. Sequences from: Oligonucleotide sequences © 2018 Illumina, Inc. All rights reserved.

Primer	Sequence, 5'-3'
S501	AATGATACGGCGACCACCGAGATCTACACTAGATCGCTCGTCGGCAGCGTC
S502	AATGATACGGCGACCACCGAGATCTACACCTCTCTATTCGTCGGCAGCGTC
S503	AATGATACGGCGACCACCGAGATCTACACTATCCTCTTCGTCGGCAGCGTC
S504	AATGATACGGCGACCACCGAGATCTACACAGAGTAGATCGTCGGCAGCGTC
S505	AATGATACGGCGACCACCGAGATCTACACGTAAGGAGTCGTCGGCAGCGTC
S506	AATGATACGGCGACCACCGAGATCTACACACTGCATATCGTCGGCAGCGTC
S507	AATGATACGGCGACCACCGAGATCTACACAAGGACTATCGTCGGCAGCGTC
S508	AATGATACGGCGACCACCGAGATCTACACCTAAGCCTTCGTCGGCAGCGTC
S510	AATGATACGGCGACCACCGAGATCTACACCGTCTAATTCGTCGGCAGCGTC
S511	AATGATACGGCGACCACCGAGATCTACACTCTCTCCGTCGTCGGCAGCGTC
S512	AATGATACGGCGACCACCGAGATCTACACTCGACTAGTCGTCGGCAGCGTC
S513	AATGATACGGCGACCACCGAGATCTACACTTCTAGCTTCGTCGGCAGCGTC
S514	AATGATACGGCGACCACCGAGATCTACACCCTAGAGTTCGTCGGCAGCGTC
S515	AATGATACGGCGACCACCGAGATCTACACGCGTAAGATCGTCGGCAGCGTC
S516	AATGATACGGCGACCACCGAGATCTACACCTATTAAGTCGTCGGCAGCGTC
S517	AATGATACGGCGACCACCGAGATCTACACAAGGCTATTCGTCGGCAGCGTC
N701	CAAGCAGAAGACGGCATACGAGATTAAGGCGAGTCTCGTGGGCTCGG
N702	CAAGCAGAAGACGGCATACGAGATCGTACTAGGTCTCGTGGGCTCGG
N703	CAAGCAGAAGACGGCATACGAGATAGGCAGAAGTCTCGTGGGCTCGG
N704	CAAGCAGAAGACGGCATACGAGATTCCTGAGCGTCTCGTGGGCTCGG
N705	CAAGCAGAAGACGGCATACGAGATGGACTCCTGTCTCGTGGGCTCGG
N706	CAAGCAGAAGACGGCATACGAGATTAGGCATGGTCTCGTGGGCTCGG
N707	CAAGCAGAAGACGGCATACGAGATGTGTGTAGGTCTCGTGGGCTCGG
N708	CAAGCAGAAGACGGCATACGAGATCAGAGAGGGTCTCGTGGGCTCGG
N709	CAAGCAGAAGACGGCATACGAGATGCTAGGGTGTCTCGTGGGCTCGG
N710	CAAGCAGAAGACGGCATACGAGATCGAGGCTGGTCTCGTGGGCTCGG
N711	CAAGCAGAAGACGGCATACGAGATAAGAGGCAGTCTCGTGGGCTCGG
N712	CAAGCAGAAGACGGCATACGAGATGTAGAGGAGTCTCGTGGGCTCGG
N713	CAAGCAGAAGACGGCATACGAGATGCTCATGAGTCTCGTGGGCTCGG
N714	CAAGCAGAAGACGGCATACGAGATATCTCAGGGTCTCGTGGGCTCGG
N715	CAAGCAGAAGACGGCATACGAGATACTCGCTAGTCTCGTGGGCTCGG
N716	CAAGCAGAAGACGGCATACGAGATGGAGCTACGTCTCGTGGGCTCGG
N717	CAAGCAGAAGACGGCATACGAGATGCGTAGTAGTCTCGTGGGCTCGG
N718	CAAGCAGAAGACGGCATACGAGATCGGAGCCTGTCTCGTGGGCTCGG
N719	CAAGCAGAAGACGGCATACGAGATTACGCTGCGTCTCGTGGGCTCGG
N720	CAAGCAGAAGACGGCATACGAGATATGCGCAGGTCTCGTGGGCTCGG
N721	CAAGCAGAAGACGGCATACGAGATTAGCGCTCGTCTCGTGGGCTCGG
N722	CAAGCAGAAGACGGCATACGAGATACTGAGCGGTCTCGTGGGCTCGG

N723	CAAGCAGAAGACGGCATACGAGATCCTAAGACGTCTCGTGGGCTCGG
N724	CAAGCAGAAGACGGCATACGAGATCGATCAGTGTCTCGTGGGCTCGG

Supplementary Table S3. Deep amplicon sequencing data of the cytochrome b locus of *T. annulata* field samples. A total of 75 positive blood samples of buffalo and 119 from cattle were collected from veterinary clinics throughout the endemic regions of Pakistan.

Buffalo isolates	Total no of Illumina MiSeq reads	Total no susceptible reads [S129(AGC), P253 (CCT), L262(TTA)]	Total no resistant reads [129G(GGT)]	Total no resistant reads [253S(TCT)]	Total no resistant reads [262S(TCA)]	Total no resistant reads [129G(GGT)/253S(TCT)]
CY107-B	12271	12271				
CY109-B	16723	16723				
CY110-B	18868	13699		5169		
CY113-B	15408	15408				
CY117-B	17350	17350				
CY123-B	46438	42178	4260			
CY126-B	12426	12426				
CY128-B	55010	55010				
CY59-B	19801	14110	5691			
CY129-B	15470	15470				
CY133-B	49042	49042				
CY138-B	70250	70250				
CY49-B	12313		12313			
CY148-B	12369	12369				
CY149-B	11077	11077				
CY157-B	13062	13062				
CY5-B	12341		12341			
CY91-B	29533	29533				
CY92-B	11236	11236				
CY96-B	15697	15697				
CY98-B	23295	23295				
CY19-B	29321	29321				
CY7-B	14489	14489				
CY8-B	16420	16420				
CY11-B	18191	18191				
CY48-B	16542		16542			
CY9-B	14130	14130				
CY97-B	17677	17677				
CY94-B	14283	14283				
CY142-B	16227	16227				
CY141-B	17489	17489				
CY139-B	19835	19835				
CY112-B	11582	11582				
CY111-B	15138	15138				
CY106-B	17127	17127				
CY4-B	21578	16127	5451			
CY60-B	15433		15433			

CY105-B	13482	13482				
CY103-B	11441	11441				
CY101-B	17165	17165				
CY47-B	17642		17642			
CY100-B	14120	14120				
CY102-B	12144	12144				
CY15-B	15662	15662				
CY16-B	13559	13559				
CY18-B	15432	15432				
CY201-B	12901	12901				
CY203-B	10787	10787				
CY205-B	16902	16902				
CY206-B	19936	19936				
CY207-B	47627	47627				
CY228-B	34864	34864				
CY254-B	12256		12256			
CY256-B	12892		12892			
CY257-B	47942		47942			
CY260-B	13314		13314			
CY261-B	23253	23253				
CY266-B	21823		21823			
CY269-B	12378		12378			
CY278-B	21004		21004			
CY282-B	74779	74779				
CY284-B	17280	17280				
CY301-B	23131	23131				
CY302-B	21227	21227				
CY304-B	43158	43158				
CY307-B	32155	32155				
CY312-B	54965	54965				
CY313-B	67781	67781				
CY317-B	14988		14988			
CY318-B	15704	15704				
CY320-B	23324		23324			
CY321-B	24581	16842	1926	4741		1072
CY322-B	102021	73077	4443	23164		1337
CY323-B	12175		12175			
CY324-B	17264	17264				

Cattle isolates	**Total no of Illumina MiSeq reads**	**Total no susceptible reads [S129(AGC), P253 (CCT), L262(TTA)]**	**Total no resistant reads [129G(GGT)]**	**Total no resistant reads [253S(TCT)]**	**Total no resistant reads [262S(TCA)]**	**Total no resistant reads [129G(GGT)/253S(TCT)]**
CY79-C	49342	49342				
CY80-C	12997	12997				
CY82-C	23106	23106				
CY83-C	64110	64110				

CY84-C	80565	80565			
CY86-C	60995	60995			
CY87-C	19526	19526			
CY88-C	16518	16518			
CY89-C	11087	11087			
CY90-C	65051	48644	10718	3948	1741
CY114-C	13491	13491			
CY119-C	80952	80952			
CY120-C	55888	55888			
CY122-C	13107	13107			
CY124-C	21450	21450			
CY130-C	26053	26053			
CY131-C	20896	20896			
CY134-C	12929	12929			
CY135-C	12083	12083			
CY136-C	23906	18706	5200		
CY140-C	4043	4043			
CY145-C	64164	64164			
CY150-C	28039	14904	3621	9514	
CY151-C	62699	62699			
CY153-C	23491	23491			
CY154-C	15483	15483			
CY155-C	21156	21156			
CY158-C	21514	21514			
CY160-C	32337	32337			
CY162-C	13576	13576			
CY163-C	23842	23842			
CY173-C	34393	34393			
CY175-C	15798	15798			
CY177-C	27292	27292			
CY1-C	21055	21055			
CY2-C	18032	18032			
CY3-C	13573	13573			
CY6-C	21001	17589	3412		
CY20-C	66615	66615			
CY22-C	22120	22120			
CY25-C	12422	12422			
CY26-C	28672	16326		12346	
CY27-C	15741	15741			
CY28-C	19559	19559			
CY29-C	12354	12354			
CY30-C	28168	28168			
CY31-C	14219	14219			
CY32-C	22304	22304			
CY33-C	13903	13903			

CY34-C	21252	21252	
CY35-C	12810	12810	
CY36-C	14812	14812	
CY37-C	47941	47941	
CY38-C	35600	2343	33257
CY39-C	45065	1999	43066
CY40-C	29245	1113	28132
CY41-C	80153	2393	77760
CY42-C	58645	1402	57243
CY44-C	12374	12374	
CY53-C	23216	23216	
CY56-C	15486	15486	
CY57-C	14224	14224	
CY43-C	12398		12398
CY195-C	13738	13738	
CY209-C	41143	41143	
CY211-C	45321	45321	
CY213-C	32161	32161	
CY214-C	56421	56421	
CY215-C	34821	34821	
CY216-C	45321	45321	
CY217-C	32412	32412	
CY219-C	32334	32334	
CY220-C	28461	28461	
CY222-C	19872	19872	
CY224-C	34408	34408	
CY225-C	38510	38510	
CY226-C	45321	45321	
CY231-C	7997	7997	
CY232-C	23731	23731	
CY233-C	35123	35123	
CY237-C	62721	62721	
CY238-C	5186	5186	
CY239-C	49316	49316	
CY240-C	66417	66417	
CY241-C	8335	8335	
CY242-C	13122	13122	
CY244-C	58077	58077	
CY246-C	36452	36452	
CY247-C	31286	31286	
CY248-C	12333	12333	
CY249-C	59818	59818	
CY250-C	57055	57055	
CY251-C	54679	54679	
CY255-C	22218	22218	

CY259-C	17832	17832			
CY262-C	18637	18637			
CY263-C	17457	17457			
CY264-C	74891	74891			
CY267-C	67308	67308			
CY271-C	23379	23379			
CY273-C	42152	42152			
CY274-C	64501	64501			
CY275-C	46299	46299			
CY276-C	47257	47257			
CY279-C	12483	12483			
CY283-C	23213	23213			
CY290-C	15466	15466			
CY295-C	29876	29876			
CY296-C	54033	54033			
CY299-C	94094	94094			
CY300-C	95517	95517			
CY305-C	81146	81146			
CY306-C	16453	16453			
CY277-C	57086	51667	1214	4205	
CY272-C	65893	60825	5068		
CY235-C	60586	47949	4318		8319
CY268-C	4483		3451	1032	
CY212-C	39057	1240	37817		
CY252-C	5173		5173		
CY270-C	79794	78497	1133	3164	
CY258-C			11512		